

A New Stabilized Finite Element Method for Advection-Diffusion-Reaction Equations

Huoyuan Duan,¹ Fengjuan Qiu²

¹School of Mathematics and Statistics, Collaborative Innovation Centre of Mathematics, Computational Science Hubei Key Laboratory, Wuhan University, Wuhan, China

²Bank of China, Beijing, China

Received 20 August 2014; accepted 26 August 2015

Published online 23 October 2015 in Wiley Online Library (wileyonlinelibrary.com).

DOI 10.1002/num.22021

In this article, a new stabilized finite element method is proposed and analyzed for advection-diffusion-reaction equations. The key feature is that both the mesh-dependent Péclet number and the mesh-dependent Damköhler number are reasonably incorporated into the newly designed stabilization parameter. The error estimates are established, where, up to the regularity-norm of the exact solution, the explicit-dependence of the diffusivity, advection, reaction, and mesh size (or the dependence of the mesh-dependent Péclet number and the mesh-dependent Damköhler number) is revealed. Such dependence in the error bounds provides a mathematical justification on the effectiveness of the proposed method for any values of diffusivity, advection, dissipative reaction, and mesh size. Numerical results are presented to illustrate the performance of the method. © 2015 Wiley Periodicals, Inc. Numer Methods Partial Differential Eq 32: 616–645, 2016

Keywords: advection-diffusion-reaction equation; boundary-layer; error estimates; large reaction; small diffusivity; stabilized finite element method

I. INTRODUCTION

As is well-known, advection-diffusion-reaction equation is a type of important model in the field of computational fluid dynamics. This model describes the development of some physical quantity (such as concentration) in the fluid flow motion. The advection-diffusion-reaction equation bears many applications in physical and environmental sciences and engineering problems. For examples, it relates to models for simulation in water pollution, semiconductor device, oil extraction from underground reservoir, flows in chemical reactors, heat transportation, etc.

Correspondence to: Huoyuan Duan, School of Mathematics and Statistics, Collaborative Innovation Centre of Mathematics, Computational Science Hubei Key Laboratory, Wuhan University, Wuhan, China (e-mail: hyduan.math@whu.edu.cn)
Contract grant sponsor: National Natural Science Foundation of China (H.D.); contract grant numbers: 11071132, 11171168, 91430106, 11571266

Contract grant sponsor: Research Fund for the Doctoral Program of Higher Education of China; contract grant numbers: 20100031110002, 20120031110026

Contract grant sponsor: Scientific Research Foundation for Returned Scholars, Ministry of Education of China
Contract grant sponsor: Fundamental Research Funds for the Central Universities (Wuhan University start-up fund); contract grant number: 2042014kf0218

© 2015 Wiley Periodicals, Inc.

In the study of finite element methods for numerically solving this type of equation, a notorious difficulty is the oscillation of the numerical solution in the boundary and inner layers [1–3]. The boundary and inner layers refer to some very narrow subregions (e.g., the immediate vicinity of the boundary) in which the exact solution or its gradient would change abruptly and drastically. In many partial differential equations arising from physical science (e.g., aerodynamics) and engineering applications (e.g., chemical engineering), the presence of boundary and inner layers are commonplace. Mathematically, the reason behind the formation of layers may be simply interpreted as the drastic discrepancy in the values of the diffusivity, the convection, and the reaction. For not sufficiently small mesh sizes, the numerical difficulty usually takes place with small diffusivity, large convection, and large reaction. For this case, the advection-diffusion-reaction equation is well-known as convection-dominated. Seeking effective and efficient finite element methods which can stably and highly accurately simulate the convection-dominated advection-diffusion-reaction equation has been and is still challenging in scientific and engineering computing. To circumvent numerical oscillations and improve stability and accuracy of the finite element solution, since as early as eighties in the last century, a large class of so-called stabilized finite element methods have been developed [4–17]. The main idea in stabilization is the augmentation of the standard Galerkin formulation with some additional terms, typically consisting of least-squares minimization of the residuals of the original partial differential equations. The additional terms may also be indirectly obtained by locally (e.g., element-by-element in the finite element triangulation) solving the original partial differential equations along with suitable local artificial boundary conditions. The stabilization may come from the bubble-enrichment method as well. In fact, some stabilizations are indeed deduced from the static condensation or elimination of the bubble functions which are usually introduced to element-locally enrich the finite element space [18–23]. The common key ingredient in all stabilizations boils down to a parameter, called as the stabilization parameter. This parameter is a formula expressing the relationship among the values of the diffusivity, the convection, the reaction, the discretization parameters (spatial mesh size, temporal time step). Physically, it locally mimics the two dimensionless numbers: Péclet number, Damköhler number. The two numbers reflect the dependence of the problem on the characteristic velocity and length scales from diffusivity, convection, and reaction. The stabilization parameter plays a key role in the stabilized finite element method. To a great degree, it accounts for why those additional terms can increase stability and enhance accuracy of the resulting finite element solution. A mathematical foundation for the role of the stabilization parameter can be found in Ref. [8]. Nowadays, stabilized finite element methods are very popular and prevalently used in the numerical solutions of partial differential equations.

Concerning the advection-diffusion-reaction equation, we may simply sort stabilization methods into two classes. One is for the advection-diffusion equations without reaction and the other for the advection-diffusion-reaction equations. Such assortment may not be quite reasonable, but, we have noticed that some stabilization methods in the first class are indeed not suitable in the presence of reaction, particularly of large reaction. For the second class, additional special stabilization techniques are often demanded, particularly in the case of large reaction. More recently, in Ref. [24], a very simple stabilized method is developed for solving the advection-diffusion-reaction equation, mainly aiming at the convection-dominated case where small diffusivity and large reaction coexist. The authors therein design a new and very simple stabilization parameter, independent of the convection field. The stabilization parameter is fixed in the given mesh, without needing to make comparisons among the magnitude of diffusivity, convection, reaction, and mesh size. Reasonable error bounds are established as well. The theoretical and numerical results show that the method in Ref. [24] can well solve the convection-dominated problem with the coexistence of small diffusivity and large reaction. For this type of problem,

standard and many other stabilized finite element methods do not work the same well. However, the defect is that for small reaction, e.g., zero reaction, the method in Ref. [24] degenerates to the standard method which is well-known not suitable for solving convection-dominated problems.

In this article, we shall propose a new stabilized finite element method for solving the advection-diffusion-reaction equation. The goal is to obtain stable and accurate finite element solution, regardless of the value of the reaction constant ranging from zero to very large. The key feature of the proposed method in this article is the new stabilization parameter that we shall design. This ad hoc parameter is designed with a well-balanced comparison among the values of the mesh size, the diffusivity, the reaction, and the convection. The stabilization parameter can also be expressed in terms of the mesh-dependent Péclet number (denoted by Pe_h) and Damköhler number (denoted by Da_h). It is well-known that Pe_h characterizes the relative magnitude among the mesh size, convection, and diffusivity, while Da_h expresses the relationship among the mesh size, convection, and reaction. It is this new stabilization parameter that the proposed method is suitable for all values of diffusive constant, convection, and dissipative reaction.

The advantages of the newly proposed method can be summarized as follows. In the case of zero advection, the method restores to the method in Ref. [22] and remains the advantages in error bounds of independence of diffusivity and reaction. For the convection-dominated case with small diffusivity and large reaction, the method is the same as the one in [24] and exhibits the same numerical merits. If the reaction is zero, the method is the Streamline-Upwind Petrov-Galerkin (SUPG) method, an excellent method for the convection-dominated advection-diffusion equation without reaction. The method of this article is thus effective for solving the general advection-diffusion-reaction equation in any regime of diffusivity, convection, and dissipative reaction. Compared with other stabilized methods such as Ref. [25] which is also very effective for the advection-diffusion-reaction equations in any regime, the method in this article is simpler (only involving the conventional residual-based stabilization terms, a simple stabilization parameter, and the standard Galerkin formulation).

By analysis, a stability with explicit dependence on diffusivity, convection, reaction, and mesh size is established. In the context of stabilized finite element methods for advection-diffusion-reaction equations, the error bounds we have obtained appears to be the first one that explicitly reveals the explicit dependence of the mesh-dependent Péclet- and Damköhler numbers (up to the regularity-norm $\|u\|_2$ of the exact solution in $H^2(\Omega)$ space), to the authors' knowledge. From this explicit dependence, a theoretical justification of the effectiveness of the proposed method follows. Optimal error bounds are also obtained, with respect to explicit dependence on diffusivity, convection, reaction, and mesh size and on the regularity of the exact solution. The error bounds provide a useful mathematical justification to support the capability of the proposed method in effectively numerically seeking a stable and accurate finite element solution of the advection-diffusion-reaction equation. Some numerical experiments are presented in this article to illustrate the performance of the proposed method.

The outline of the remainder of this article is as follows. In section 2, the advection-diffusion-reaction equation is reviewed, with a simple background addressed. In section 3, the standard Galerkin finite element is reviewed, with a numerical evidence on why the standard method fails for the convection-dominated problem of small diffusivity. In section 4, the new stabilized finite element method of this article is proposed and the stability is analyzed. In section 5, error bounds are established. In section 6, numerical experiments are performed. In the last section, concluding remarks are given.

II. ADVECTION-DIFFUSION-REACTION EQUATION

Let $\Omega \subset \mathbb{R}^2$ be a polygonal convex bounded domain, with its boundary denoted by $\partial\Omega$. We shall consider the following advection-diffusion-reaction equation:

$$\begin{cases} \mathcal{L}u := -\varepsilon \Delta u + \mathbf{a} \cdot \nabla u + \sigma u = f & \text{in } \Omega, \\ u = 0 & \text{on } \partial\Omega, \end{cases} \quad (1)$$

where u is the unknown quantity to be solved, such as concentration, $\varepsilon > 0$ is the diffusive constant, $\mathbf{a} = \mathbf{a}(x, y) \in \mathbb{R}^2$ is the convection field (i.e., the fluid velocity) which is assumed to be divergence-free ($\mathbf{a} \in (L^\infty(\Omega))^2$, $\nabla \cdot \mathbf{a} = 0$), $\sigma \geq 0$ is the dissipative reaction constant, and $f \in L^2(\Omega)$ the source function.

In the usual sense, we refer to (1) as convection-dominated by the situation where the diffusivity ε is smaller than the convection \mathbf{a} in their magnitude. The most interesting situation is the coexistence of small diffusivity and large reaction. The better measurements for being responsible for the numerical difficulties incurred in finite element methods are the mesh-dependent Péclet number and the mesh-dependent Damköhler number. These two numerical numbers will be defined later.

A derivation of the reaction term in (1) is often from the time discretization of the transient advection-diffusion equations. In that case, σ is proportionally inverse to the time-step (denoted by δt). Indeed, the common finite element approach to transient advection-diffusion equations is based on semidiscrete formulations where only the spatial dependence is approximated by finite element methods, and the resulting stiff system is then discretized by applying finite differences in time domain to obtain a fully discrete problem [26]. For problems involving fast chemical reactions, a small time step is needed in order to account for the stiffness due to the fast reactions [27]. As it has pointed out in Ref. [27] that for sufficiently small time steps and implicit time discretization, the fully discrete problem at each time level is analog to the finite element approximation of the convection-dominated problem (1) with large reaction.

III. STANDARD GALERKIN FINITE ELEMENT METHOD

To state the variational problem of (1), we shall adopt the standard Sobolev spaces in [28]. On $H_0^1(\Omega) \times H_0^1(\Omega)$, define the bilinear form:

$$B(u, v) := \varepsilon(\nabla u, \nabla v) + (\mathbf{a} \cdot \nabla u, v) + \sigma(u, v),$$

where (\cdot, \cdot) denotes L^2 -inner product. On $H_0^1(\Omega)$, define the linear form:

$$L(v) := (f, v).$$

Thus, the standard variational problem reads as follows:

$$\begin{cases} \text{Find } u \in H_0^1(\Omega), \text{ such that} \\ B(u, v) = L(v), \forall v \in H_0^1(\Omega). \end{cases} \quad (2)$$

The standard Galerkin finite element method for (2) is introduced in the following. First, let $\{\mathcal{T}_h\}_{0 < h \leq 1}$ denote the shape-regular triangulation of $\overline{\Omega}$ into triangles. A generic triangle element is denoted as T , with the diameter h_T . The mesh size $h := \max_{T \in \mathcal{T}_h} h_T$.

Define the finite element space $U_h \subset H_0^1(\Omega)$, a standard finite dimensional space of continuous piecewise polynomials with respect to \mathcal{T}_h . In this article, we choose

$$U_h := \{v \in H_0^1(\Omega) : v|_T \in P_1(T), \forall T \in \mathcal{T}_h\}, \quad (3)$$

where $P_1(T)$ denotes the space of linear polynomials over T . According to the classical theory of finite elements [29, 30], for $u \in H_0^1(\Omega) \cap H^2(\Omega)$, there exists an interpolation $\Pi_h u \in U_h$, such that

$$\|u - \Pi_h u\|_0 + h|u - \Pi_h u|_1 \leq Ch^2\|u\|_2. \quad (4)$$

The standard Galerkin finite element method is stated as the following problem:

$$\begin{cases} \text{Find } u_h \in U_h, \text{ such that} \\ B(u_h, v) = L(v), \forall v \in U_h. \end{cases} \quad (5)$$

IV. A NEW STABILIZED FINITE ELEMENT METHOD

In this section, we shall propose a new finite element method for (1). This method employs the same finite element space as before. The finite element formulation is different. It will consist of an additional stabilization term, with an ad hoc stabilization parameter.

We first state the new stabilized finite element method of (1), called as *New stabilized FEM*:

$$\begin{cases} \text{Find } u_h \in U_h, \text{ such that} \\ B_h(u_h, v) = L_h(v), \forall v \in U_h. \end{cases} \quad (6)$$

In the above, the bilinear form $B_h(u, v)$ and the linear form $L_h(v)$ are defined as follows:

$$B_h(u, v) := B(u, v) - \sum_{T \in \mathcal{T}_h} \tau (\mathcal{L}u, -\varepsilon \Delta v - \xi \mathbf{a} \cdot \nabla v + \sigma v)_T, \quad (7)$$

$$L_h(v) := L(v) - \sum_{T \in \mathcal{T}_h} \tau (f, -\varepsilon \Delta v - \xi \mathbf{a} \cdot \nabla v + \sigma v)_T, \quad (8)$$

where $(\cdot, \cdot)_T$ denotes the L^2 -inner product over T . The stabilization parameter τ is defined as follows:

$$\tau := \frac{h^2}{\sigma h^2 + h|\mathbf{a}|_\infty \xi + 6\varepsilon}, \quad (9)$$

where

$$\xi = \begin{cases} 0 & , \text{ if } \frac{|\mathbf{a}|_\infty}{\sigma h} \leq 1; \\ 1 & , \text{ if } \frac{|\mathbf{a}|_\infty}{\sigma h} > 1 \text{ and } \frac{h|\mathbf{a}|_\infty}{\varepsilon} < 1; \\ \frac{\varepsilon}{h|\mathbf{a}|_\infty} & , \text{ if } \frac{|\mathbf{a}|_\infty}{\sigma h} > 1 \text{ and } \frac{h|\mathbf{a}|_\infty}{\varepsilon} \geq 1, \end{cases} \quad (10)$$

where $|\boldsymbol{a}|_\infty$ is defined as follows:

$$|\boldsymbol{a}|_\infty := \begin{cases} \sqrt{a_1^2 + a_2^2} & , \text{ if } \boldsymbol{a} \text{ is constant vector-valued;} \\ \max_{(x,y) \in \Omega} \sqrt{a_1(x,y)^2 + a_2(x,y)^2} & , \text{ if } \boldsymbol{a} \text{ is vector-valued function depending} \\ & \text{on the } xy\text{-coordinates.} \end{cases}$$

Define the mesh-dependent Péclet number Pe_h and the mesh-dependent Damköhler number Da_h as follows:

$$Pe_h := \frac{h|\boldsymbol{a}|_\infty}{\varepsilon}, \quad Da_h := \frac{\sigma h}{|\boldsymbol{a}|_\infty} \quad (\text{if } \boldsymbol{a} \neq \mathbf{0}). \quad (11)$$

With these numerical numbers, the stabilization parameter can be restated as follows:

$$\tau := \frac{h^2}{\sigma h^2 + \varepsilon Pe_h \xi + 6\varepsilon}, \quad (12)$$

where

$$\xi = \begin{cases} 0 & , \text{ if } Da_h \geq 1; \\ 1 & , \text{ if } Da_h < 1 \text{ and } Pe_h < 1; \\ \frac{1}{Pe_h} & , \text{ if } Da_h < 1 \text{ and } Pe_h \geq 1. \end{cases} \quad (13)$$

We have seen that the stabilization parameter deeply roots in the physical problem itself, through locally embodying the Péclet number and the Damköhler number.

If $\boldsymbol{a} = \mathbf{0}$, then τ will be simply taken as

$$\tau = \frac{h^2}{\sigma h^2 + 6\varepsilon}. \quad (14)$$

Note that there is a constant number “6” in τ . This is because, if $\boldsymbol{a} = \mathbf{0}$, (14) can also be obtained from the *mini* element method by the standard procedure of static elimination of the enriched-bubble. Such a procedure generates the constant “6.” The *mini* element is the enrichment of the standard linear element by one element-bubble.

Some remarks are given below for the stabilization parameter defined as above.

- i. If $Da_h \geq 1$, then τ reduces to the one in Ref. [24]. This case ensures that (6) can still work well for the convection-dominated problem with small diffusivity and large reaction (i.e., large Da_h).
- ii. If $Da_h < 1$ is small (even zero when $\sigma = 0$) and $Pe_h \geq 1$, then τ takes the very simple form:

$$\frac{h^2}{\sigma h^2 + 7\varepsilon}, \quad (15)$$

and the additional term in $B_h(u, v)$ becomes

$$-\sum_{T \in \mathcal{T}_h} \tau (\mathcal{L}u, -\varepsilon \Delta v - \xi \boldsymbol{a} \cdot \nabla v + \sigma v)_T$$

$$= - \sum_{T \in \mathcal{T}_h} \frac{h^2}{\sigma h^2 + 7\varepsilon} \left(\mathcal{L}u, -\varepsilon \Delta v - \frac{\varepsilon}{h|\mathbf{a}|_\infty} \mathbf{a} \cdot \nabla v + \sigma v \right)_T.$$

If $\sigma = 0$, this stabilization reduces to the one in SUPG method, e.g., see [13]. Consequently, even if $\sigma = 0$, (6) performs well for the convection-dominated problem with small diffusivity, i.e., with large Pe_h .

For the case $\sigma \neq 0$, the above stabilization, together with the stabilization parameter (15), is not seen elsewhere.

- iii. If $Da_h < 1$ is small and $Pe_h < 1$, this is the trivial case for which the standard Galerkin method can perform well. In this case, the stabilization is a type of \mathcal{LL}^* or adjoint stabilization approach, and looks like the well-known Galerkin Least/Squares approach. In the case $\mathbf{a} = \mathbf{0}$, for example, the method (6) is the one in Ref. [22], with the stabilization parameter (14).

Indeed, the stabilization method in (6) is somehow a type of adjoint stabilization, up to a factor ξ .

The stabilization parameter (11)–(13) (or (9)–(10)) and the stabilization (7) and (8) are new, as far as we know. Because the *New stabilized FEM* (6), with (11)–(13) (or (9)–(10)) and (7) and (8), incorporates the mesh-dependent Péclet number Pe_h and the mesh-dependent Damköhler number Da_h into the finite element formulation, one can expect that (6) will be suitable for all cases of the advection-diffusion-reaction equation with different order of magnitude in the parameters: $h, \varepsilon, \mathbf{a}, \sigma$. In the next section, error analysis will be carried out in details. The error bounds we shall obtain give the mathematical justification why (6) can perform well regardless of the values that the parameters $h, \varepsilon, \mathbf{a}, \sigma$.

In what follows, we give a quite obvious stability of the *New stabilized FEM* (6).

From (7), we can first have the coercivity.

Lemma 1. *For all $v \in U_h$, we have*

$$\begin{aligned} B_h(v, v) &= \varepsilon \|\nabla v\|_0^2 + \sigma \|v\|_0^2 + \tau \xi \|\mathbf{a} \cdot \nabla v\|_0^2 - \tau \sigma^2 \|v\|_0^2 \\ &= \varepsilon \|\nabla v\|_0^2 + \tau \xi \|\mathbf{a} \cdot \nabla v\|_0^2 + \frac{\sigma h |\mathbf{a}|_\infty \xi + 6\sigma \varepsilon}{\sigma h^2 + h |\mathbf{a}|_\infty \xi + 6\varepsilon} \|v\|_0^2. \end{aligned} \quad (16)$$

Proof. Since $\nabla \cdot \mathbf{a} = 0$, we have $(\mathbf{a} \cdot \nabla v, v) = 0$ for all $v \in U_h$. From (7), applying Green formula of integration by parts, with direct simplifications, we obtain (16). ■

It follows from Lemma 1 that $B_h(u, v)$ is coercive, and it is also obvious continuous over U_h , with respect to the following mesh-dependent *energy norm* $\|\cdot\|_h$:

$$\|v\|_h = (B_h(v, v))^{1/2} = \left(\varepsilon \|\nabla v\|_0^2 + \tau \xi \|\mathbf{a} \cdot \nabla v\|_0^2 + \frac{\sigma h |\mathbf{a}|_\infty \xi + 6\sigma \varepsilon}{\sigma h^2 + h |\mathbf{a}|_\infty \xi + 6\varepsilon} \|v\|_0^2 \right)^{1/2}. \quad (17)$$

In the case of advection-diffusion equation with $\sigma = 0$, the norm on the convection term is $\tau \xi \|\mathbf{a} \cdot \nabla v\|_0^2$. For a dominated convection (i.e., $\frac{h|\mathbf{a}|_\infty}{\varepsilon} \geq 1$ and $\xi = \frac{\varepsilon}{h|\mathbf{a}|_\infty}$), up to different multiplicative constants, this norm is the same as the ones in the literature [5, 9], while for a dominated diffusion (i.e., $\frac{h|\mathbf{a}|_\infty}{\varepsilon} < 1$ and $\xi = 1$), this norm with a factor $h^2/(h|\mathbf{a}|_\infty + 6\varepsilon)$ is a little bit different from the ones in Refs. [5, 9], e.g., the one in Ref. [5] with a factor $h^2/(12\varepsilon)$.

Theorem 1. *The New stabilized FEM (6) admits a unique solution $u_h \in U_h$, satisfying the stability estimation:*

$$|||u_h|||_h \leq C \max \left(\frac{(h|\mathbf{a}|_\infty \xi + 6\epsilon)\epsilon^{-\frac{1}{2}}}{\sigma h^2 + h|\mathbf{a}|_\infty \xi + 6\epsilon}, \tau^{\frac{1}{2}} \xi^{\frac{1}{2}} \right) ||f||_0. \quad (18)$$

Proof. The existence and uniqueness of the solution can be trivially concluded from Lemma 1 and the classical Lax–Milgram lemma [29, 30]. One can easily obtain the stability (18), noting the fact that

$$L_h(v) = \frac{(h|\mathbf{a}|_\infty \xi + 6\epsilon)(f, v)}{\sigma h^2 + h|\mathbf{a}|_\infty \xi + 6\epsilon} - \tau \xi(f, \mathbf{a} \cdot \nabla v).$$

■

To see the stability in (18) in a clearer way, we consider the cases for $\xi = 0, 1/Pe_h, 1$, as defined in (10). First, if $\xi = 0$, we have

$$||\nabla u_h||_0 \leq \frac{C}{\sigma h^2 + 6\epsilon} ||f||_0. \quad (19)$$

Second, if $\xi = 1/Pe_h$ where $\mathbf{a} \neq \mathbf{0}$, we have

$$||\nabla u_h||_0 \leq C \max \left(\frac{1}{\sigma h^2 + 7\epsilon}, \frac{h}{\sqrt{\sigma h^2 + 7\epsilon} \sqrt{h|\mathbf{a}|_\infty}} \right) ||f||_0. \quad (20)$$

Third, if $\xi = 1$, i.e., $h < \min(\frac{\epsilon}{|\mathbf{a}|_\infty}, \frac{|\mathbf{a}|_\infty}{\sigma})$ where $\mathbf{a} \neq \mathbf{0}$, we have

$$||\nabla u_h||_0 \leq C \max \left(\frac{1}{\sigma h^2 + h|\mathbf{a}|_\infty + 6\epsilon}, \frac{\epsilon^{-\frac{1}{2}} h}{\sqrt{\sigma h^2 + h|\mathbf{a}|_\infty + 6\epsilon}} \right) ||f||_0. \quad (21)$$

In the discretization of time-dependent problem, as is well-known that the time-step $\delta t (= C\sigma^{-1})$ is usually taken as h^2 (e.g., see Ref. [31]). For this situation, we can easily see that, for all cases of ξ ,

$$||\nabla u_h||_0 \leq C ||f||_0. \quad (22)$$

This is a uniform stability, with respect to $h, \epsilon, \mathbf{a}, \sigma$.

In addition, we notice that the *New stabilized FEM* (6) is consistent. Denote by u denote the exact solution of (2). We find that u satisfies (6), i.e., $B_h(u, v_h) = L_h(v_h), \forall v_h \in U_h$. As a consequence, the error orthogonality holds:

$$B_h(u - u_h, v) = 0, \forall v \in U_h. \quad (23)$$

V. ERROR ESTIMATES

In this section, we shall analyze the errors between the finite element solution and the exact solution. The error bounds which will be established reveal the explicit dependence on the mesh-dependent Péclet number Pe_h and Damköhler number Da_h . Consequently, why the proposed method can well simulate the advection-diffusion-reaction equation is theoretically justified.

Lemma 2. *Let $u \in H_0^1(\Omega)$, satisfying $u \in H^2(\Omega)$, denote the solution of problem (1). For this u , we define a source function*

$$\tilde{f} := -\varepsilon \Delta u + \sigma u.$$

Let $\rho_h u$ denote the finite element solution to New stabilized FEM (6), but with $\mathbf{a} = \mathbf{0}$ and with the source function \tilde{f} . That is to say, $\rho_h u \in U_h$ satisfies

$$\begin{aligned} & \varepsilon(\nabla \rho_h u, \nabla v) + \sigma(\rho_h u, v) - \sum_{T \in \mathcal{T}_h} \tau(-\varepsilon \Delta \rho_h u + \sigma \rho_h u, -\varepsilon \Delta v + \sigma v)_T \\ &= (\tilde{f}, v) - \sum_{T \in \mathcal{T}_h} \tau(\tilde{f}, -\varepsilon \Delta v + \sigma v)_T \\ &= \varepsilon(\nabla u, \nabla v) + \sigma(u, v) - \sum_{T \in \mathcal{T}_h} \tau(-\varepsilon \Delta u + \sigma u, -\varepsilon \Delta v + \sigma v)_T, \forall v \in U_h. \end{aligned} \quad (24)$$

Then, there exists a constant $C > 0$, independent of ε, σ, h , such that

$$\|u - \rho_h u\|_1 \leq Ch\|u\|_2, \quad (25)$$

$$\|u - \rho_h u\|_0 \leq Ch^2\|u\|_2. \quad (26)$$

Proof. For $\mathbf{a} = \mathbf{0}$, we have $\tau = \frac{h^2}{\sigma h^2 + 6\varepsilon}$ and

$$\|v\|_h = (B_h(v, v))^{1/2} = \left(\varepsilon \|\nabla v\|_0^2 + \frac{6\sigma\varepsilon}{\sigma h^2 + 6\varepsilon} \|v\|_0^2 \right)^{1/2}. \quad (27)$$

Let $e_h = \Pi_h u - \rho_h u$, where $\Pi_h u \in U_h$ is the classical finite element interpolation of u , and let $\eta_1 = u - \rho_h u$. From the error orthogonality (23) and the trivial fact that $\Delta e_h = 0$, $e_h \in U_h$, we have

$$\begin{aligned} \|e_h\|_h^2 &= B_h(e_h, e_h) = B_h(\Pi_h u - \rho_h u, e_h) = B_h(\Pi_h u - u, e_h) \\ &= \varepsilon(\nabla(\Pi_h u - u), \nabla e_h) + \sigma(\Pi_h u - u, e_h) \\ &\quad - \sum_{T \in \mathcal{T}_h} \tau(-\varepsilon \Delta(\Pi_h u - u) + \sigma(\Pi_h u - u), -\varepsilon \Delta e_h + \sigma e_h)_T \\ &= \varepsilon(\nabla(\Pi_h u - u), \nabla e_h) + (\sigma - \tau\sigma^2)(\Pi_h u - u, e_h) + \tau\sigma\varepsilon \sum_{T \in \mathcal{T}_h} (\Delta(\Pi_h u - u), e_h)_T. \end{aligned}$$

By the Cauchy–Schwarz inequality and the finite element interpolation error estimates (4), we have

$$\begin{aligned}
 |||e_h|||^2_h &= \varepsilon(\nabla(\Pi_h u - u), \nabla e_h) + (\sigma - \tau\sigma^2)(\Pi_h u - u, e_h) + \tau\sigma\varepsilon \sum_{T \in \mathcal{T}_h} (\Delta(\Pi_h u - u), e_h)_T \\
 &\leq \varepsilon ||\nabla(\Pi_h u - u)||_0 ||\nabla e_h||_0 + \frac{\sigma\varepsilon 6}{\sigma h^2 + 6\varepsilon} ||\Pi_h u - u||_0 ||e_h||_0 \\
 &\quad + \frac{\varepsilon\sigma h^2}{\sigma h^2 + 6\varepsilon} \left(\sum_{T \in \mathcal{T}_h} ||\Delta(\Pi_h u - u)||_{0,T}^2 \right)^{\frac{1}{2}} ||e_h||_0 \\
 &\leq Ch\varepsilon ||u||_2 ||\nabla e_h||_0 + Ch^2 \frac{\sigma\varepsilon 6}{\sigma h^2 + 6\varepsilon} ||u||_2 ||e_h||_0 + \frac{C\varepsilon\sigma h^2}{\sigma h^2 + 6\varepsilon} ||u||_2 ||e_h||_0 \\
 &\leq Ch\sqrt{\varepsilon} ||u||_2 ||e_h||_h + Ch^2 \sqrt{\frac{\sigma\varepsilon 6}{\sigma h^2 + 6\varepsilon}} ||u||_2 ||e_h||_h + Ch^2 \frac{\sqrt{\varepsilon\sigma}}{\sqrt{\sigma h^2 + 6\varepsilon}} ||u||_2 ||e_h||_h \\
 &\leq C \left(h\sqrt{\varepsilon} + \frac{h^2\sqrt{\varepsilon\sigma}}{\sqrt{\sigma h^2 + 6\varepsilon}} \right) ||u||_2 ||e_h||_h,
 \end{aligned}$$

that is,

$$|||e_h|||_h \leq C \left(h\sqrt{\varepsilon} + \frac{h^2\sqrt{\varepsilon\sigma}}{\sqrt{\sigma h^2 + 6\varepsilon}} \right) ||u||_2. \quad (28)$$

From (27) and (28), we have

$$\sqrt{\varepsilon} ||\nabla e_h||_0 \leq C \left(h\sqrt{\varepsilon} + \frac{h^2\sqrt{\varepsilon\sigma}}{\sqrt{\sigma h^2 + 6\varepsilon}} \right) ||u||_2.$$

Dividing by $\sqrt{\varepsilon}$ in both sides of the above, we have

$$||\nabla e_h||_0 \leq C \left(h + \frac{h^2\sqrt{\sigma}}{\sqrt{\sigma h^2 + 6\varepsilon}} \right) ||u||_2 \leq Ch ||u||_2. \quad (29)$$

Since $||\nabla e_h||_0$ is equivalent to $||e_h||_1$, by the triangle inequality and (4), we obtain (25) from

$$||\eta_1||_1 = ||u - \rho_h u||_1 \leq ||u - \Pi_h u||_1 + ||e_h||_1 \leq Ch ||u||_2.$$

Similarly, from (27) and (28), we have

$$\frac{\sqrt{\sigma}}{\sqrt{\sigma h^2 + 6\varepsilon}} ||e_h||_0 \leq Ch ||u||_2.$$

By the triangle inequality and (4), we have

$$\begin{aligned}
 \frac{\sqrt{\sigma}}{\sqrt{\sigma h^2 + 6\varepsilon}} ||u - \rho_h u||_0 &\leq \frac{\sqrt{\sigma}}{\sqrt{\sigma h^2 + 6\varepsilon}} (||u - \Pi_h u||_0 + ||\Pi_h u - \rho_h u||_0) \\
 &\leq \frac{\sqrt{\sigma}}{\sqrt{\sigma h^2 + 6\varepsilon}} Ch^2 ||u||_2 + Ch ||u||_2 \\
 &\leq Ch ||u||_2.
 \end{aligned} \quad (30)$$

In what follows, we will apply the classical Aubin–Nitsche duality argument [29, 30], to continue to prove $\|u - \rho_h u\|_0 \leq Ch^2 \|u\|_2$. Taking $u - \rho_h u$ as the source function, we consider the auxiliary problem:

$$\begin{cases} -\varepsilon \Delta \theta + \sigma \theta = u - \rho_h u, \\ \theta|_\Gamma = 0. \end{cases} \quad (31)$$

Since Ω is convex, from Refs. [32, 33] we can have the regularity of θ as follows:

$$\begin{aligned} \sigma \|\theta\|_0 &\leq \|u - \rho_h u\|_0, \\ \varepsilon \|\nabla \theta\|_0 &\leq C \|u - \rho_h u\|_0, \\ \|\theta\|_2 &\leq C \|\Delta \theta\|_0 \leq C \varepsilon^{-1} \|u - \rho_h u\|_0, \end{aligned} \quad (32)$$

where the constant C does not depend on ε, σ .

Introduce the classical finite element interpolation $\Pi_h \theta \in U_h$ of θ , denoted by θ_h . Noticing that $\eta_1 = u - \rho_h u$, from (31) and (24) with $v := \theta_h$, noting that $\Delta \theta_h = 0$ and $\Delta \eta_1 = \Delta u$ on T , we have

$$\begin{aligned} \|\eta_1\|_0^2 &= (-\varepsilon \Delta \theta + \sigma \theta, \eta_1) = \varepsilon (\nabla \theta, \nabla \eta_1) + \sigma (\theta, \eta_1) \\ &= \varepsilon (\nabla (\theta - \theta_h), \nabla \eta_1) + \sigma (\theta - \theta_h, \eta_1) - \sum_{T \in \mathcal{T}_h} \tau (-\varepsilon \Delta \theta_h + \sigma \theta_h, -\varepsilon \Delta \eta_1 + \sigma \eta_1)_T \\ &\quad + \varepsilon (\nabla \theta_h, \nabla \eta_1) + \sigma (\theta_h, \eta_1) + \sum_{T \in \mathcal{T}_h} \tau (-\varepsilon \Delta \theta_h + \sigma \theta_h, -\varepsilon \Delta \eta_1 + \sigma \eta_1)_T \\ &= \varepsilon (\nabla (\theta - \theta_h), \nabla \eta_1) + \sigma (\theta - \theta_h, \eta_1) - \sum_{T \in \mathcal{T}_h} \tau (\sigma (\theta - \theta_h), -\varepsilon \Delta u + \sigma \eta_1)_T \\ &\quad + \sum_{T \in \mathcal{T}_h} \tau (\sigma \theta, -\varepsilon \Delta u + \sigma \eta_1)_T \\ &= \varepsilon (\nabla (\theta - \theta_h), \nabla \eta_1) + \frac{\sigma \varepsilon h^2}{\sigma h^2 + 6\varepsilon} (\Delta u, \theta - \theta_h) \\ &\quad + \frac{\sigma \varepsilon 6}{\sigma h^2 + 6\varepsilon} (\theta - \theta_h, \eta_1) - \frac{\varepsilon \sigma h^2}{\sigma h^2 + 6\varepsilon} (\Delta u, \theta) + \frac{\sigma^2 h^2}{\sigma h^2 + 6\varepsilon} (\theta, \eta_1), \end{aligned}$$

where, by the Cauchy–Schwarz inequality,

$$\begin{aligned} \|\eta_1\|_0^2 &\leq \varepsilon \|\nabla (\theta - \theta_h)\|_0 \|\nabla \eta_1\|_0 + \frac{\sigma \varepsilon h^2}{\sigma h^2 + 6\varepsilon} \|\Delta u\|_0 \|\theta - \theta_h\|_0 \\ &\quad + \frac{\sigma \varepsilon 6}{\sigma h^2 + 6\varepsilon} \|\theta - \theta_h\|_0 \|\eta_1\|_0 + \frac{\varepsilon \sigma h^2}{\sigma h^2 + 6\varepsilon} \|\Delta u\|_0 \|\theta\|_0 + \frac{\sigma^2 h^2}{\sigma h^2 + 6\varepsilon} \|\theta\|_0 \|\eta_1\|_0, \end{aligned}$$

and thus, from (4), (25), and (30), we have

$$\begin{aligned} \|\eta_1\|_0^2 &\leq Ch^2 \varepsilon \|\theta\|_2 \|u\|_2 + \frac{C \sigma h^4}{\sigma h^2 + 6\varepsilon} \varepsilon \|\theta\|_2 \|u\|_2 \\ &\quad + \frac{Ch^3 \sqrt{\sigma}}{\sqrt{\sigma h^2 + 6\varepsilon}} \varepsilon \|\theta\|_2 \|u\|_2 + \frac{C \varepsilon h^2}{\sigma h^2 + 6\varepsilon} \sigma \|\theta\|_0 \|u\|_2 + \frac{Ch^3 \sqrt{\sigma}}{\sqrt{\sigma h^2 + 6\varepsilon}} \sigma \|\theta\|_0 \|u\|_2, \end{aligned}$$

By virtue of the regularity in (32), we have

$$\begin{aligned}
\|\eta_1\|_0^2 &\leq Ch^2\|\eta_1\|_0\|u\|_2 + \frac{C\sigma h^4}{\sigma h^2 + 6\varepsilon}\|u\|_2\|\eta_1\|_0 \\
&+ \frac{Ch^3\sqrt{\sigma}}{\sqrt{\sigma}h^2 + 6\varepsilon}\|\eta_1\|_0\|u\|_2 + \frac{C\varepsilon h^2}{\sigma h^2 + 6\varepsilon}\|\eta_1\|_0\|u\|_2 + \frac{Ch^3\sqrt{\sigma}}{\sqrt{\sigma}h^2 + 6\varepsilon}\|\eta_1\|_0\|u\|_2 \\
&\leq C\left(h^2 + \frac{\sigma h^4}{\sigma h^2 + 6\varepsilon} + \frac{h^3\sqrt{\sigma}}{\sqrt{\sigma}h^2 + 6\varepsilon} + \frac{\varepsilon h^2}{\sigma h^2 + 6\varepsilon}\right)\|\eta_1\|_0\|u\|_2 \\
&\leq Ch^2\|\eta_1\|_0\|u\|_2,
\end{aligned}$$

that is,

$$\|\eta_1\|_0 \leq Ch^2\|u\|_2.$$

Therefore, (26) holds true. The proof is thus completed. \blacksquare

This lemma will play a key intermediate step in the establishment of the following error estimates. We should point out that the good property in both (25) and (26) is that, up to the $\|u\|_2$ norm, both (25) and (26) are uniform in both ε and σ .

Lemma 3. *For $\mathbf{a} \neq \mathbf{0}$, let $u_h \in U_h$ denote the finite element solution of New stabilized FEM (6), and let $\rho_h u \in U_h$ denote the finite element interpolation as a projection defined in Lemma 2. Then, there exists a constant $C > 0$, independent of ε, σ, h , such that*

$$\|\rho_h u - u_h\|_1 \leq \begin{cases} Ch\|u\|_2 & , \xi = 0; \\ Ch\|u\|_2 & , \xi = 1; \\ Ch\left(1 + \sqrt{\frac{Pe_h}{Da_h Pe_h + 7}}\right)\|u\|_2 & , \xi = \frac{1}{Pe_h}; \end{cases} \quad (33)$$

$$\|\rho_h u - u_h\|_0 \leq \begin{cases} Ch^2\|u\|_2 & , \xi = 0; \\ Ch^2\left(1 + \frac{1}{\sqrt{Da_h}\sqrt{Pe_h}}\right)\|u\|_2 & , \xi = 1; \\ Ch^2\left(1 + \frac{1}{\sqrt{Da_h}}\right)\|u\|_2 & , \xi = \frac{1}{Pe_h}. \end{cases} \quad (34)$$

Proof. Put $\eta_2 = \rho_h u - u_h$. By the energy norm (17), the error orthogonality (23), the trivial fact that $\Delta\eta_2 = 0$ and $\Delta\rho_h u = 0$, and the definition of $\rho_h u$ in (24), we have

$$\begin{aligned}
\|\eta_2\|_h^2 &= B_h(\eta_2, \eta_2) = B_h(\rho_h u - u + u - u_h, \eta_2) = B_h(\rho_h u - u, \eta_2) \\
&= \varepsilon(\nabla(\rho_h u - u), \nabla\eta_2) + (\mathbf{a} \cdot \nabla(\rho_h u - u), \eta_2) + \sigma(\rho_h u - u, \eta_2) \\
&- \sum_{T \in \mathcal{T}_h} \tau(-\varepsilon\Delta(\rho_h u - u) + \mathbf{a} \cdot \nabla(\rho_h u - u) + \sigma(\rho_h u - u), -\xi\mathbf{a} \cdot \nabla\eta_2 + \sigma\eta_2)_T \\
&= \frac{\varepsilon(h|\mathbf{a}|_\infty\varepsilon^{-1}\xi + 6)}{\sigma h^2 + h|\mathbf{a}|_\infty\xi + 6\varepsilon}(\mathbf{a} \cdot \nabla(\rho_h u - u), \eta_2) \\
&+ \xi\tau(\varepsilon\Delta u + \mathbf{a} \cdot \nabla(\rho_h u - u) + \sigma(\rho_h u - u), \mathbf{a} \cdot \nabla\eta_2). \tag{35}
\end{aligned}$$

To estimate the right-hand side of (35), we shall discuss case-by-case in the following.

1. If $\xi = 0$, i.e., $Da_h \geq 1$, from the Cauchy–Schwarz inequality and Lemma 2, we have

$$\begin{aligned} (\mathbf{a} \cdot \nabla(\rho_h u - u), \eta_2) &= (u - \rho_h u, \mathbf{a} \cdot \nabla \eta_2) \leq \|u - \rho_h u\|_0 \|\mathbf{a} \cdot \nabla \eta_2\|_0 \\ &\leq Ch^2 |\mathbf{a}|_\infty \|u\|_2 \|\nabla \eta_2\|_0. \end{aligned}$$

From the definition of $\|\eta_2\|_h$, we have

$$\varepsilon \|\nabla \eta_2\|_0^2 \leq \|\eta_2\|_h^2 = \frac{6\varepsilon}{\sigma h^2 + 6\varepsilon} (\mathbf{a} \cdot \nabla(\rho_h u - u), \eta_2) \leq C \frac{6\varepsilon}{\sigma h^2 + 6\varepsilon} h^2 |\mathbf{a}|_\infty \|u\|_2 \|\nabla \eta_2\|_0.$$

Dividing by $\varepsilon \|\nabla \eta_2\|_0$ to both side in the above, we have

$$\|\nabla \eta_2\|_0 \leq \frac{6}{\sigma h^2 + 6\varepsilon} Ch^2 |\mathbf{a}|_\infty \|u\|_2 \leq C \frac{h}{Da_h} \|u\|_2 \leq Ch \|u\|_2. \quad (36)$$

From the Young's inequality, we have

$$\begin{aligned} \|u - \rho_h u\|_0 \|\nabla \eta_2\|_0 &\leq \frac{\delta}{2} \|u - \rho_h u\|_0^2 + \frac{1}{2\delta} \|\nabla \eta_2\|_0^2 \quad \left(\text{where } \delta := \frac{3|\mathbf{a}|_\infty}{\sigma h^2} \right) \\ &= \frac{3|\mathbf{a}|_\infty}{2\sigma h^2} \|u - \rho_h u\|_0^2 + \frac{\sigma h^2}{6|\mathbf{a}|_\infty} \|\nabla \eta_2\|_0^2. \end{aligned}$$

From the definition of $\|\eta_2\|_h$ and (35), we have

$$\begin{aligned} \varepsilon \|\nabla \eta_2\|_0^2 + \frac{6\sigma\varepsilon}{\sigma h^2 + 6\varepsilon} \|\eta_2\|_0^2 &= \frac{6\varepsilon}{\sigma h^2 + 6\varepsilon} (\mathbf{a} \cdot \nabla(\rho_h u - u), \eta_2) \\ &\leq \frac{6\varepsilon}{\sigma h^2 + 6\varepsilon} |\mathbf{a}|_\infty \frac{3|\mathbf{a}|_\infty}{2\sigma h^2} \|u - \rho_h u\|_0^2 \\ &\quad + \frac{6\varepsilon}{\sigma h^2 + 6\varepsilon} |\mathbf{a}|_\infty \frac{\sigma h^2}{6|\mathbf{a}|_\infty} \|\nabla \eta_2\|_0^2, \end{aligned}$$

and we have

$$\begin{aligned} \frac{6\sigma\varepsilon}{\sigma h^2 + 6\varepsilon} \|\eta_2\|_0^2 &\leq \frac{6\varepsilon}{\sigma h^2 + 6\varepsilon} \frac{3|\mathbf{a}|_\infty^2}{2\sigma h^2} \|u - \rho_h u\|_0^2 + \left(\frac{\varepsilon\sigma h^2}{\sigma h^2 + 6\varepsilon} - \varepsilon \right) \|\nabla \eta_2\|_0^2 \\ &= \frac{6\varepsilon}{\sigma h^2 + 6\varepsilon} \frac{3|\mathbf{a}|_\infty^2}{2\sigma h^2} \|u - \rho_h u\|_0^2 - \frac{6\varepsilon^2}{\sigma h^2 + 6\varepsilon} \|\nabla \eta_2\|_0^2 \\ &\leq \frac{6\varepsilon}{\sigma h^2 + 6\varepsilon} \frac{3|\mathbf{a}|_\infty^2}{2\sigma h^2} \|u - \rho_h u\|_0^2. \end{aligned}$$

Dividing by $\frac{6\sigma\varepsilon}{\sigma h^2 + 6\varepsilon}$ to both sides of the above, and taking the square root, applying Lemma 2, we have

$$\|\eta_2\|_0 \leq C \frac{|\mathbf{a}|_\infty}{\sigma h} h^2 \|u\|_2 \leq C \frac{h^2}{Da_h} \|u\|_2 \leq Ch^2 \|u\|_2. \quad (37)$$

1. If $\xi \neq 0$, $Da_h < 1$, by amplification and minification to each term in the right-hand side of (35), from Lemma 2, we have

$$\begin{aligned} \sigma h^2 &= \sigma hh = Da_h |\mathbf{a}|_\infty h < |\mathbf{a}|_\infty h, \\ (\mathbf{a} \cdot \nabla(\rho_h u - u), \eta_2) &= (u - \rho_h u, \mathbf{a} \cdot \nabla \eta_2) \leq C(\xi \tau)^{-1/2} h^2 \|u\|_2 (\xi \tau)^{1/2} \|\mathbf{a} \cdot \nabla \eta_2\|_0, \\ \xi \tau \varepsilon(\Delta u, \mathbf{a} \cdot \nabla \eta_2) &\leq C\varepsilon(\xi \tau)^{1/2} \|u\|_2 (\xi \tau)^{1/2} \|\mathbf{a} \cdot \nabla \eta_2\|_0, \\ \xi \tau (\mathbf{a} \cdot \nabla(\rho_h u - u), \mathbf{a} \cdot \nabla \eta_2) &\leq C(\xi \tau)^{1/2} |\mathbf{a}|_\infty h \|u\|_2 (\xi \tau)^{1/2} \|\mathbf{a} \cdot \nabla \eta_2\|_0, \\ \xi \tau \sigma(\rho_h u - u, \mathbf{a} \cdot \nabla \eta_2) &= -\xi \tau \sigma(\mathbf{a} \cdot \nabla(\rho_h u - u), \eta_2) \\ &\leq C(\xi h^2 \sqrt{\tau \sigma} |\mathbf{a}|_\infty) (h |\mathbf{a}|_\infty \xi + 6\varepsilon)^{-1/2} \|u\|_2 h^{-1} \sqrt{\tau \sigma (h |\mathbf{a}|_\infty \xi + 6\varepsilon)} \|\eta_2\|_0. \end{aligned}$$

From the definition of $\|\eta_2\|_h$, we have

$$\sqrt{\varepsilon} \|\nabla \eta_2\|_0 \leq \|\eta_2\|_h, \quad (\tau \xi)^{1/2} \|\mathbf{a} \cdot \nabla \eta_2\|_0 \leq \|\eta_2\|_h, \quad \sqrt{\frac{\sigma h |\mathbf{a}|_\infty \xi + 6\varepsilon \sigma}{\sigma h^2 + h |\mathbf{a}|_\infty \xi + 6\varepsilon}} \|\eta_2\|_0 \leq \|\eta_2\|_h.$$

Hence

$$\begin{aligned} \|\eta_2\|_h^2 &\leq C \left(\frac{\varepsilon(h |\mathbf{a}|_\infty \varepsilon^{-1} \xi + 6)}{\sigma h^2 + h |\mathbf{a}|_\infty \xi + 6\varepsilon} (\xi \tau)^{-1/2} h^2 + \varepsilon(\xi \tau)^{1/2} + (\xi \tau)^{1/2} |\mathbf{a}|_\infty h + \frac{\xi h^2 \sqrt{\tau \sigma} |\mathbf{a}|_\infty}{\sqrt{h |\mathbf{a}|_\infty \xi + 6\varepsilon}} \right) \\ &\quad \times \|u\|_2 \|\eta_2\|_h, \end{aligned}$$

that is

$$\begin{aligned} \|\eta_2\|_h &\leq C \left(\frac{\varepsilon(h |\mathbf{a}|_\infty \varepsilon^{-1} \xi + 6)}{\sigma h^2 + h |\mathbf{a}|_\infty \xi + 6\varepsilon} (\xi \tau)^{-1/2} h^2 + \varepsilon(\xi \tau)^{1/2} + (\xi \tau)^{1/2} |\mathbf{a}|_\infty h + \frac{\xi h^2 \sqrt{\tau \sigma} |\mathbf{a}|_\infty}{\sqrt{h |\mathbf{a}|_\infty \xi + 6\varepsilon}} \right) \\ &\quad \times \|u\|_2, \end{aligned} \tag{38}$$

Therefore, from the definition of $\|\eta_2\|_h$ and the definition (9) of τ , we have

$$\begin{aligned} \|\nabla \eta_2\|_0 &\leq C \left(\frac{\sqrt{\varepsilon}(6 + h |\mathbf{a}|_\infty \varepsilon^{-1} \xi) \xi^{-\frac{1}{2}} h}{\sqrt{\sigma h^2 + h |\mathbf{a}|_\infty \xi + 6\varepsilon}} + \frac{\sqrt{\varepsilon} \xi^{\frac{1}{2}} h}{\sqrt{\sigma h^2 + h |\mathbf{a}|_\infty \xi + 6\varepsilon}} \right. \\ &\quad \left. + \frac{\varepsilon^{-\frac{1}{2}} \xi^{\frac{1}{2}} |\mathbf{a}|_\infty h^2}{\sqrt{\sigma h^2 + h |\mathbf{a}|_\infty \xi + 6\varepsilon}} + \frac{\varepsilon^{-\frac{1}{2}} \xi h^3 |\mathbf{a}|_\infty \sqrt{\sigma}}{\sqrt{\sigma h^2 + h |\mathbf{a}|_\infty \xi + 6\varepsilon} \sqrt{h |\mathbf{a}|_\infty \xi + 6\varepsilon}} \right) \|u\|_2, \end{aligned} \tag{39}$$

$$\begin{aligned} \|\eta_2\|_0 &\leq C \left(\frac{\sqrt{\varepsilon} \xi^{-\frac{1}{2}} \sqrt{h |\mathbf{a}|_\infty \varepsilon^{-1} \xi + 6}}{\sqrt{\sigma}} h + \frac{\sqrt{\varepsilon} \xi^{\frac{1}{2}} h}{\sqrt{\sigma} \sqrt{h |\mathbf{a}|_\infty \varepsilon^{-1} \xi + 6}} \right. \\ &\quad \left. + \frac{\xi^{\frac{1}{2}} |\mathbf{a}|_\infty h^2}{\sqrt{\sigma} \sqrt{h |\mathbf{a}|_\infty \varepsilon^{-1} \xi + 6}} + \frac{\sqrt{\sigma} h^3 \xi |\mathbf{a}|_\infty}{\sqrt{\sigma} \sqrt{h |\mathbf{a}|_\infty \varepsilon^{-1} \xi + 6} \sqrt{h |\mathbf{a}|_\infty \xi + 6\varepsilon}} \right) \|u\|_2. \end{aligned} \tag{40}$$

(2.1) If $\xi = 1$, with $0 \leq Pe_h = \frac{h |\mathbf{a}|_\infty}{\varepsilon} < 1$, $0 \leq Da_h = \frac{\sigma h}{|\mathbf{a}|_\infty} < 1$, i.e.,

$$h |\mathbf{a}|_\infty < \varepsilon, \quad \sigma h < |\mathbf{a}|_\infty, \quad \sigma h^2 < h |\mathbf{a}|_\infty < \varepsilon,$$

and $6\varepsilon < \sigma h^2 + h|\mathbf{a}|_\infty + 6\varepsilon < 8\varepsilon$, $6 \leq 6 + Pe_h < 7$. Thus, substituting $\xi = 1$ into (39), (40), and doing some simplifications, we have

$$\begin{aligned} \|\nabla \eta_2\|_0 &\leq C \left(\frac{\sqrt{\varepsilon}(6 + Pe_h)h}{\sqrt{\sigma h^2 + h|\mathbf{a}|_\infty + 6\varepsilon}} + \frac{\sqrt{\varepsilon}h}{\sqrt{\sigma h^2 + h|\mathbf{a}|_\infty + 6\varepsilon}} \right. \\ &\quad \left. + \frac{\sqrt{\varepsilon}Pe_hh}{\sqrt{\sigma h^2 + h|\mathbf{a}|_\infty + 6\varepsilon}} + \frac{\sqrt{\varepsilon}hPe_h\sqrt{\sigma h^2}}{\sqrt{\sigma h^2 + h|\mathbf{a}|_\infty + 6\varepsilon}\sqrt{h|\mathbf{a}|_\infty + 6\varepsilon}} \right) \|u\|_2 \\ &\leq Ch\|u\|_2, \end{aligned} \quad (41)$$

$$\begin{aligned} \|\eta_2\|_0 &\leq C \left(\frac{\sqrt{\varepsilon}\sqrt{Pe_h+6}}{\sqrt{\sigma}}h + \frac{\sqrt{\varepsilon}h}{\sqrt{\sigma}\sqrt{Pe_h+6}} \right. \\ &\quad \left. + \frac{|\mathbf{a}|_\infty h^2}{\sqrt{\sigma\varepsilon}\sqrt{Pe_h+6}} + \frac{\sqrt{\sigma}h^3|\mathbf{a}|_\infty}{\sqrt{\sigma\varepsilon}\sqrt{Pe_h+6}\sqrt{h|\mathbf{a}|_\infty + 6\varepsilon}} \right) \|u\|_2 \\ &\leq C \left(h^2 + \frac{\sqrt{\varepsilon}}{\sqrt{\sigma}}h \right) \|u\|_2 \\ &\leq Ch^2 \left(1 + \frac{1}{\sqrt{Da_h}\sqrt{Pe_h}} \right) \|u\|_2. \end{aligned} \quad (42)$$

(2.2) If $\xi = \frac{1}{Pe_h}$, with $Pe_h = \frac{h|\mathbf{a}|_\infty}{\varepsilon} \geq 1$ or $h|\mathbf{a}|_\infty \geq \varepsilon$ and $Da_h = \frac{\sigma h}{|\mathbf{a}|_\infty} < 1$ or $\sigma h < |\mathbf{a}|_\infty$. Substituting $\xi = \frac{1}{Pe_h}$ into (39), (40), doing some simplifications, we have

$$\begin{aligned} \|\nabla \eta_2\|_0 &\leq C \left(\frac{\sqrt{\varepsilon} \left(6 + Pe_h \frac{1}{Pe_h} \right) \left(\frac{1}{Pe_h} \right)^{-\frac{1}{2}} h}{\sqrt{\sigma h^2 + h|\mathbf{a}|_\infty \frac{1}{Pe_h} + 6\varepsilon}} + \frac{\sqrt{\varepsilon} \left(\frac{1}{Pe_h} \right)^{\frac{1}{2}} h}{\sqrt{\sigma h^2 + h|\mathbf{a}|_\infty \frac{1}{Pe_h} + 6\varepsilon}} \right. \\ &\quad \left. + \frac{\varepsilon^{-\frac{1}{2}} \left(\frac{1}{Pe_h} \right)^{\frac{1}{2}} |\mathbf{a}|_\infty h^2}{\sqrt{\sigma h^2 + h|\mathbf{a}|_\infty \frac{1}{Pe_h} + 6\varepsilon}} + \frac{\varepsilon^{-\frac{1}{2}} \frac{1}{Pe_h} h^3 |\mathbf{a}|_\infty \sqrt{\sigma}}{\sqrt{\sigma h^2 + h|\mathbf{a}|_\infty \frac{1}{Pe_h} + 6\varepsilon} \sqrt{h|\mathbf{a}|_\infty \frac{1}{Pe_h} + 6\varepsilon}} \right) \|u\|_2 \quad (1) \\ &\leq C \left(\frac{7\sqrt{\varepsilon}\sqrt{h|\mathbf{a}|_\infty}h}{\sqrt{\sigma h^2 + 7\varepsilon}\sqrt{\varepsilon}} + \frac{\sqrt{\varepsilon}\sqrt{\varepsilon}h}{\sqrt{\sigma h^2 + 7\varepsilon}\sqrt{h|\mathbf{a}|_\infty}} \right. \\ &\quad \left. + \frac{\varepsilon^{-\frac{1}{2}}\sqrt{\varepsilon}|\mathbf{a}|_\infty h^2}{\sqrt{\sigma h^2 + 7\varepsilon}\sqrt{|\mathbf{a}|_\infty h}} + \frac{\varepsilon^{-\frac{1}{2}}\varepsilon h^2\sqrt{\sigma}}{\sqrt{\sigma h^2 + 7\varepsilon}\sqrt{7\varepsilon}} \right) \|u\|_2 \\ &\leq C \left(\frac{h\sqrt{h|\mathbf{a}|_\infty}}{\sqrt{\sigma h^2 + 7\varepsilon}} + h \right) \|u\|_2 = Ch \left(1 + \sqrt{\frac{Pe_h}{Da_h Pe_h + 7}} \right) \|u\|_2, \end{aligned} \quad (43)$$

$$\|\eta_2\|_0 \leq C \left(\frac{\sqrt{\varepsilon} \left(\frac{1}{Pe_h} \right)^{-\frac{1}{2}} \sqrt{Pe_h \frac{1}{Pe_h} + 6}}{\sqrt{\sigma}} h + \frac{\sqrt{\varepsilon} \left(\frac{1}{Pe_h} \right)^{\frac{1}{2}} h}{\sqrt{\sigma} \sqrt{Pe_h \frac{1}{Pe_h} + 6}} \right)$$

$$\begin{aligned}
& + \left(\frac{\left(\frac{1}{Pe_h}\right)^{\frac{1}{2}} |\mathbf{a}|_\infty h^2}{\sqrt{\sigma\varepsilon} \sqrt{Pe_h \frac{1}{Pe_h} + 6}} + \frac{\sqrt{\sigma} h^3 \frac{1}{Pe_h} |\mathbf{a}|_\infty}{\sqrt{\sigma\varepsilon} \sqrt{Pe_h \frac{1}{Pe_h} + 6} \sqrt{h |\mathbf{a}|_\infty \frac{1}{Pe_h} + 6\varepsilon}} \right) ||u||_2 \\
& \leq C \left(\frac{\sqrt{\varepsilon} \sqrt{h |\mathbf{a}|_\infty} h}{\sqrt{\sigma} \sqrt{\varepsilon}} + \frac{\sqrt{\varepsilon} \sqrt{\varepsilon} h}{\sqrt{\sigma} \sqrt{h |\mathbf{a}|_\infty}} + \frac{\sqrt{\varepsilon} \sqrt{h |\mathbf{a}|_\infty} h}{\sqrt{\sigma} \sqrt{\varepsilon}} + \frac{\sqrt{\sigma} h^2 \varepsilon}{\sqrt{\sigma} \sqrt{\varepsilon} \sqrt{7\varepsilon}} \right) ||u||_2 \\
& \leq C \left(\frac{h \sqrt{h} |\mathbf{a}|_\infty}{\sqrt{\sigma}} + \frac{\varepsilon h}{\sqrt{\sigma} h |\mathbf{a}|_\infty} + h^2 \right) ||u||_2 \\
& \leq Ch^2 \left(1 + \frac{1}{\sqrt{Da_h}} \right) ||u||_2. \tag{44}
\end{aligned}$$

With (36), (37), (41), (42), (43), and (44), thus, the proof completes. ■

Theorem 2. Let $u_h \in U_h$ denote the finite element solution of (6). Let $u \in H_0^1(\Omega)$ and $u \in H^2(\Omega)$ be the exact solution of problem (1). Then, there exists a constant $C > 0$, independent of ε, σ, h , such that

$$||u - u_h||_1 \leq \begin{cases} Ch ||u||_2 & , \xi = 0; \\ Ch ||u||_2 & , \xi = 1; \\ Ch \left(1 + \sqrt{\frac{Pe_h}{Da_h Pe_h + 7}} \right) ||u||_2 & , \xi = \frac{1}{Pe_h}. \end{cases} \tag{45}$$

$$||u - u_h||_0 \leq \begin{cases} Ch^2 ||u||_2 & , \xi = 0; \\ Ch^2 \left(1 + \frac{1}{\sqrt{Da_h} \sqrt{Pe_h}} \right) ||u||_2 & , \xi = 1; \\ Ch^2 \left(1 + \frac{1}{\sqrt{Da_h}} \right) ||u||_2 & , \xi = \frac{1}{Pe_h}. \end{cases} \tag{46}$$

Proof. By the triangle inequality, we have

$$||u - u_h||_1 \leq ||u - \rho_h u||_1 + ||\rho_h u - u_h||_1,$$

$$||u - u_h||_0 \leq ||u - \rho_h u||_0 + ||\rho_h u - u_h||_0,$$

and from Lemma 2 and Lemma 3, it follows that (45) and (46) hold. The proof is thus completed. ■

The error bounds in (45) and (46) can ensure that the finite element solution $u_h \in U_h$ of (6) converges to u , both in H^1 norm and L^2 norm, for h tends to zero. We have seen that, so long as $\sigma \neq 0$ (i.e., $Da_h \neq 0$), the L^2 -norm error bounds are already one-order higher than those H^1 -semi norm error bounds. Note that, in the case $\xi = \frac{1}{Pe_h}$, the H^1 norm error bound can obviously become

$$||u - u_h||_1 \leq Ch \left(1 + \frac{1}{\sqrt{Da_h}} \right) ||u||_2.$$

On the other hand, for any $\sigma \geq 0$, applying the classical Aubin–Nitsche duality argument, one can obtain an L^2 -norm error bound with one-order higher than the H^1 -seminorm error bound. We leave this to the interested readers.

In what follows, we give several observations.

- i. In particular, for the case $\xi = 0$, i.e., $\sigma h \geq |\mathbf{a}|_\infty$, relative to h , the error bound in H^1 norm reaches the optimum $O(h)$ and the error bound in L^2 norm the optimum $O(h^2)$. This justifies that (6) is suitable for the problem with large Damköhler number Da_h and does not depend on Péclet number Pe_h . In other words, in the case of large Damköhler number Da_h , whatsoever $\varepsilon > 0$, \mathbf{a} and h take their values, the resultant finite element solution behaves like the finite element interpolation (best approximation).
- ii. In the case where $\xi = 1$, i.e., $\sigma h < |\mathbf{a}|_\infty$ and $h|\mathbf{a}|_\infty < \varepsilon$, the error bound in H^1 norm reaches $O(h)$ the optimum, still not depending on the magnitude of Péclet number Pe_h . The error bound in L^2 norm approximates $O(h^2)$ the optimum, depending on Péclet number Pe_h and Damköhler number Da_h . Interestingly, note that

$$Pe_h Da_h = \frac{\sigma h^2}{\varepsilon}. \quad (47)$$

The error bound in L^2 norm becomes:

$$\|u - u_h\|_0 \leq Ch^2 \left(1 + \frac{1}{\sqrt{Da_h} \sqrt{Pe_h}} \right) \|u\|_2 \leq Ch^2 \left(1 + \sqrt{\frac{\varepsilon}{\sigma h^2}} \right) \|u\|_2. \quad (48)$$

If

$$\varepsilon \leq \sigma h^2, \quad (49)$$

we immediately obtain

$$\|u - u_h\|_0 \leq Ch^2 \|u\|_2. \quad (50)$$

We should point out that (49) usually holds true. In fact, $\sigma = \frac{1}{\delta t}$, where δt being the time step is taken as h^2 (see [31]). Then, (49) is satisfied with $\varepsilon \leq 1$.

- iii. In the case $\xi = \frac{1}{Pe_h}$, i.e., $\sigma h < |\mathbf{a}|_\infty$ and $\varepsilon \leq h|\mathbf{a}|_\infty$, the error bounds in H^1 norm and L^2 norm approximate the optimum, explicitly depending on the mesh-dependent Péclet number Pe_h and Damköhler number Da_h . If $\sigma = 0$, the obtained error bound (45) in H^1 -norm is comparable to the one in [34]. Note that the *New stabilized FEM* (6) is the same as the SUPG method for the case $\sigma = 0$. Interestingly, one can see that, under (49) and $\sigma h^2 = 1$, we have

$$\|u - u_h\|_0 + h\|u - u_h\|_1 \leq Ch^2(1 + \sqrt{h|\mathbf{a}|_\infty})\|u\|_2.$$

Before closing this section, we should give several remarks.

The analysis in this article is inspired by the one in [24]. In our paper, the analysis is more general, e.g., we are dealing with the test function with convection in the stabilization term; in our paper, we also establish a more refined and better results, comparing the error bound results in Theorem 2 of our paper with the results in Theorem 4 and Remark 4 of Ref. [24]; in our paper, we have provided a better L2 error estimates. Moreover, in [24], no results are available for the case $\sigma = 0$. Most importantly, the method in this paper is novel, more applicable, and performs better than the method in Ref. [24].

The stabilization parameter is fixed and element-independent, but we only assume shape-regular meshes. First, if either $\sigma = 0$ or $\mathbf{a} = \mathbf{0}$, local stabilization parameter can be of course

employed and all the theoretical results hold. Second, if using a local stabilization parameter, i.e., replacing h by h_T and $|\mathbf{a}|_\infty$ by $|\mathbf{a}|_{\infty,T}$ in (9) and (10), for the situation $\sigma \neq 0$, one cannot establish the so neatly good stability in Lemma 1, because $(\mathbf{a} \cdot \nabla v_h, v_h)_{0,T}$ cannot be annihilated locally. Below is a more detailed explanation for this. The reason why we use a global τ is to deal with both the convection and the reaction by annihilating some terms in two aspects. One is that the global parameter allows to annihilate the term $\tau \sum_{T \in \mathcal{T}_h} (\mathbf{a} \cdot \nabla v, \sigma v)_T = \tau \sigma (\mathbf{a} \cdot \nabla v, v) = 0$ so that we can obtain a better stability result. See Lemma 1. If τ is element-wise defined, this term cannot be annihilated. The other is that, in error estimates, we can combine the term $(\mathbf{a} \cdot \nabla (\rho_h u - u), \eta_2)$ with the term from the stabilization $\tau \sum_{T \in \mathcal{T}_h} (\mathbf{a} \cdot \nabla (\rho_h u - u), \sigma \eta_2)_T$ so that we can have a desirable factor ε . Please see the first term in the last terms in Eq. (35). If τ is element-wise defined, we have no way to obtain a factor ε in estimating the error term $(\mathbf{a} \cdot \nabla (\rho_h u - u), \eta_2)$. Thus, it is due to this global definition of the parameter τ that, up to the regularity norm $\|u\|_2$ of the exact solution, we can obtain the ε -independent error bounds in the first two terms (corresponding to the two cases $\xi = 0$ and $\xi = 1$) in the right-hand side of Eq. (45) in Theorem 2. Note that, in the literature (e.g., see [25]), the error bound is usually measured in an ε -weighted $H^1(\Omega)$ -norm, i.e., in terms of the standard $H^1(\Omega)$ -norm without any weights, the error bound depends on both an explicit factor $\varepsilon^{-1/2}$ as well as the regularity norm $\|u\|_2$ of the exact solution. Even in the case $\xi = 1/Pe_h$, i.e., the often-seen convection-dominated case with $Pe_h \geq 1$ and $Da_h < 1$, the result is also desirable, e.g., if $\sigma = 0$, we have $\|u - u_h\|_1 \leq \left(Ch + C \frac{h^{\frac{3}{2}} |\mathbf{a}|_\infty^{\frac{1}{2}}}{\varepsilon^{\frac{1}{2}}} \right) \|u\|_2$.

On the other hand, the fixed parameter somehow thwarts the use of adaptive meshes. However, as is often seen in the literature of stabilized finite element methods, adaptive mesh computations seem to be generally unnecessary for an effective stabilized finite element method, because accurate results can be already obtained for boundary or/and interior layer problems, e.g., see the numerical experiments in [24] and in the next section of this article; see also further [13, 14] for addressing this issue.

Also, the stabilization parameter (9) is only designed for the linear (or bilinear) element. If the higher-order finite elements are used, since $\Delta v_h \neq 0$ for $v_h \in U_h$, the stabilization parameter in the method needs to be modified as follows:

$$\tau := \frac{\alpha h^2}{\alpha \sigma h^2 + h |\mathbf{a}|_\infty \xi + 6\varepsilon}, \quad (51)$$

where the constant α is used for ensuring the coercivity and can be determined from the inverse estimates

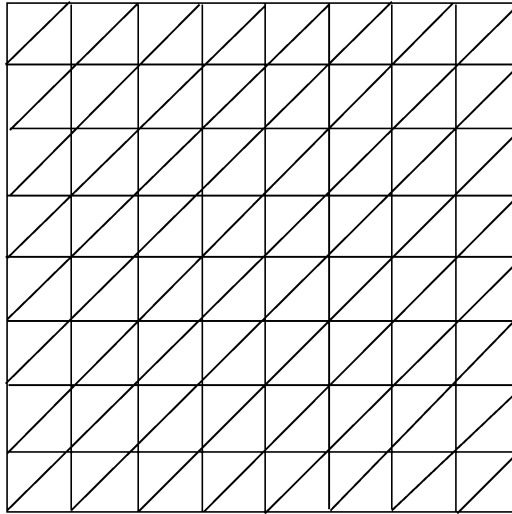
$$\|\Delta v_h\|_{0,T} \leq C \|\nabla v_h\|_{0,T} \quad \forall T \in \mathcal{T}_h, \forall v_h \in U_h. \quad (52)$$

Based on our numerical experience, a more general (and possibly more effective) stabilization parameter would be

$$\tau := \frac{\alpha h^2}{\alpha \sigma h^2 + h |\mathbf{a}|_\infty \xi_\beta + \gamma \varepsilon}, \quad (53)$$

where

$$\xi_\beta = \begin{cases} 0 & , \text{if } \frac{|\mathbf{a}|_\infty}{\sigma h} \leq 1; \\ 1 & , \text{if } \frac{|\mathbf{a}|_\infty}{\sigma h} > 1 \text{ and } \frac{h |\mathbf{a}|_\infty}{\varepsilon} < 1; \\ \frac{\beta \varepsilon}{h |\mathbf{a}|_\infty} & , \text{if } \frac{|\mathbf{a}|_\infty}{\sigma h} > 1 \text{ and } \frac{h |\mathbf{a}|_\infty}{\varepsilon} \geq 1, \end{cases} \quad (54)$$

FIG. 1. Uniform triangle triangulation: $h^* = 1/8$.

and α, β, γ are constants which may depend on the order of approximations but independent of $h, \sigma, \varepsilon, \mathbf{a}$. For this general stabilization parameter, the previous stability and error analysis still remain valid. In the next section, since we will use linear elements, $\alpha = \beta = \gamma = 1$ can work in theory. However, we choose $\alpha = 1, \beta = 7$ and $\gamma = 6$ to observe better numerical performance. The reason is not theoretically known for why the choices of $\beta = 7$ and $\gamma = 6$ lead to better numerical results than the choices $\beta = 1$ and $\gamma = 1$.

We also observed that how to define the mesh size would also affect the approximation quality of the finite element solutions. In fact, it is suggested in [35] that, under the presence of convection ($\mathbf{a} \neq \mathbf{0}$), the largest element diameter should be computed in the direction of \mathbf{a} , in order to obtain better numerical results. Such a computation is also chosen in Ref. [24] and actually much improve the finite element solutions. So, since we use uniform meshes in the next section, the largest mesh size in the direction of \mathbf{a} is denoted as $h = h_T$, while the standard mesh size is taken as h^* which is defined in section 3.

VI. NUMERICAL EXPERIMENTS

In this section, four numerical examples (including a time-dependent problem) are performed to illustrate the performance of the proposed method. In these examples, the boundary and/or inner layers present. The first example is used to confirm the theoretical error bounds obtained in the previous section. The computed in the second example are used to confirm the claim that the method is suitable for $\sigma = 0$. In the third example, a time-dependent problem which contains the transport is considered. The last example is to illustrate the performance of the proposed method on unstructured and nonuniform meshes. In this example, a comparison is made with the well-known SUPG method. Readers may refer to Ref. [36] for more numerical results.

We use Matlab to program to perform the numerical simulation. Choose $\Omega := (0, 1) \times (0, 1)$. The triangulation is uniform triangles, the standard mesh size is taken as $h^* = 2^{-l}$, l is the integer not less than 1. In Fig. 1, the triangulation of uniform triangles with $h^* = 1/8$ is given.

TABLE I. Péclet number Pe_h for different ε .

ε	$h^* = 1/32$	$h^* = 1/64$	$h^* = 1/128$	$h^* = 1/256$
10^{-1}	0.36084392	0.18042196	0.09021098	0.04510549
10^{-2}	3.60843918	1.80421959	0.90210980	0.45105490

TABLE II. Damköhler number Da_h for different σ .

σ	$h^* = 1/32$	$h^* = 1/64$	$h^* = 1/128$	$h^* = 1/256$
10^{-2}	0.00036084	0.00018042	0.00009021	0.00004511
10^{-1}	0.00360844	0.00180422	0.00090211	0.00045105
10^0	0.03608439	0.01804220	0.00902110	0.00451055
10^1	0.36084392	0.18042196	0.09021098	0.04510549
10^2	3.60843918	1.80421959	0.90210980	0.45105490

TABLE III. When $\varepsilon = 10^{-1}$, relative errors in L^2 norm under different values of σ .

σ	$h^* = 1/32$	$h^* = 1/64$	$h^* = 1/128$	$h^* = 1/256$	Order
10^{-2}	0.01092456	0.00280182	0.00070890	0.00017825	1.97916458
10^{-1}	0.01092250	0.00280113	0.00070870	0.00017820	1.97921531
10^0	0.01092039	0.00279956	0.00070816	0.00017805	1.97954203
10^1	0.01125522	0.00288964	0.00073132	0.00018391	1.97849361
10^2	0.01248305	0.00317748	0.00082717	0.00020836	1.96825633

TABLE IV. When $\varepsilon = 10^{-2}$, relative errors in L^2 norm under different values of σ .

σ	$h^* = 1/32$	$h^* = 1/64$	$h^* = 1/128$	$h^* = 1/256$	Order
10^{-2}	0.08439229	0.03273533	0.01324457	0.00356135	1.52220486
10^{-1}	0.08449708	0.03275678	0.01323896	0.00355975	1.52301752
10^0	0.08554057	0.03296762	0.01318640	0.00354479	1.53094602
10^1	0.09431878	0.03465818	0.01286280	0.00345352	1.59046888
10^2	0.11140194	0.03611437	0.01261124	0.00340832	1.67685712

A. Example 1: Exact Solution is Known

In this example, the exact solution of problem (1) is taken as follows:

$$u(x, y) = \left(\frac{x^2}{2a_1} + \frac{\varepsilon x}{a_1^2} + \left(\frac{1}{2a_1} + \frac{\varepsilon}{a_1^2} \right) \frac{e^{\frac{-a_1}{\varepsilon}} - e^{\frac{-a_1(1-x)}{\varepsilon}}}{1 - e^{\frac{-a_1}{\varepsilon}}} \right) \times \left(\frac{y^2}{2a_2} + \frac{\varepsilon y}{a_2^2} + \left(\frac{1}{2a_2} + \frac{\varepsilon}{a_2^2} \right) \frac{e^{\frac{-a_2}{\varepsilon}} - e^{\frac{-a_2(1-y)}{\varepsilon}}}{1 - e^{\frac{-a_2}{\varepsilon}}} \right),$$

and the convection field (fluid velocity) $\mathbf{a} = (a_1, a_2)^T := (1/2, \sqrt{3}/2)^T$. It can be verified that $u|_{\partial\Omega} = 0$. Define the relative errors e_{L^2} in L^2 norm and e_{H^1} in H^1 norm as follows: $e_{L^2} = \|u - u_h\|_0 / \|u\|_0$ and $e_{H^1} = \|u - u_h\|_1 / \|u\|_1$. Take $\sigma = 10^{m_1}, -2 \leq m_1 \leq 2$, and $\varepsilon = 10^{-m_2}, 1 \leq m_2 \leq 2$, where m_1, m_2 are two integers. The mesh-dependent Péclet number Pe_h s and Damköhler number Da_h s are computed in Tables I and II, respectively. The computed results of L^2 norm and H^1 norm are listed in Tables III–VI. Note that the largest element size in the direction of \mathbf{a} is $h = \sqrt{4/3}h^*$ and is used in the computation of the stabilization parameter.

TABLE V. When $\varepsilon = 10^{-1}$, relative errors in H^1 norm under different values of σ .

σ	$h^* = 1/32$	$h^* = 1/64$	$h^* = 1/128$	$h^* = 1/256$	Order
10^{-2}	0.10768438	0.05402862	0.02703663	0.01352103	0.99784391
10^{-1}	0.10768500	0.05402871	0.02703665	0.01352103	0.99784664
10^0	0.10769246	0.05402978	0.02703679	0.01352105	0.99787927
10^1	0.10779187	0.05404465	0.02703878	0.01352131	0.99831388
10^2	0.10847392	0.05414809	0.02705439	0.01352335	1.00127475

TABLE VI. When $\varepsilon = 10^{-2}$, relative errors in H^1 norm under different values of σ .

σ	$h^* = 1/32$	$h^* = 1/64$	$h^* = 1/128$	$h^* = 1/256$	Order
10^{-2}	0.53339113	0.32710467	0.17752328	0.08982492	0.85666871
10^{-1}	0.53330585	0.32711046	0.17752159	0.08982467	0.85659316
10^0	0.53253641	0.32716906	0.17750596	0.08982240	0.85591102
10^1	0.52959535	0.32776351	0.17742773	0.08981297	0.85329828
10^2	0.53339896	0.32883196	0.17781903	0.08992959	0.85611572

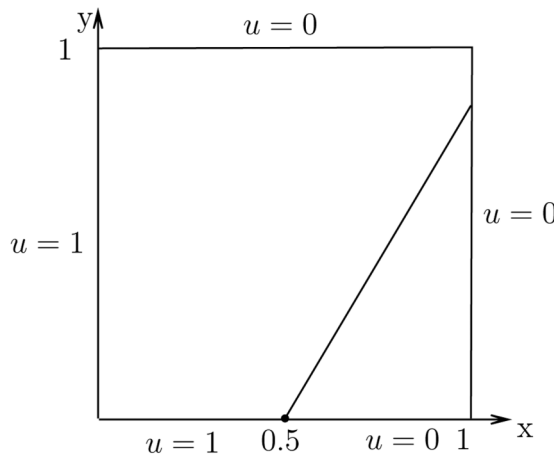


FIG. 2. Domain and boundary data of example 2.

From the formula $\log_2(||u - u_{2h^*}||_m / ||u - u_{h^*}||_m)$, where $m = 0, 1$, we can obtain an order, and then compute the average of these orders. In all the tables from Tables III–VI, the order is the average. The conclusion can be drawn in the following:

From Tables III and V, we can see that when $\varepsilon = 0.1$, *New stabilized FEM* (6) exhibits the optimal error bound $O(h)$ in H^1 norm, well consistent with the predicted in Theorem 2 in the case where $Pe_h < 1$; while the computed error bound in L^2 norm also reaches the optimum $O(h^2)$, confirming the predicted in Theorem 2.

From Tables IV and VI, we can see that when $\varepsilon = 0.01$, *New stabilized FEM* (6) also exhibits the optimal error bound $O(h)$ in H^1 norm in the case where $Da_h \geq 1$ or in the case where $0 \leq Da_h < 1, 0 \leq Pe_h < 1$. In the case where $Da_h < 1, 1 \leq Pe_h$, the error bound in H^1 norm approximates the optimum $O(h)$, mimicking the predicted in Theorem 2; while the error bound in L^2 norm approaches to the optimum $O(h^2)$, basically consistent with the predicted in Theorem 2.

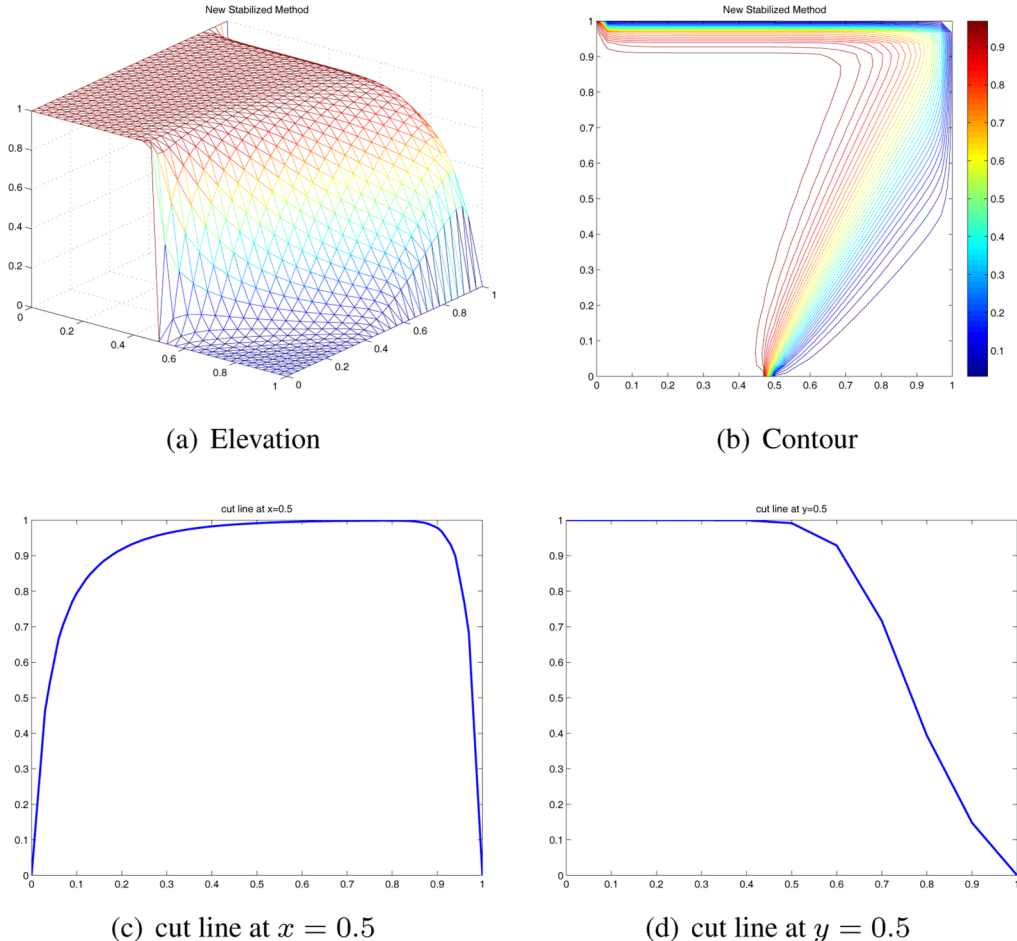


FIG. 3. The elevation, contour, and vertical and horizontal cuts of the finite element solution, with $\varepsilon = 10^{-2}$, $\mathbf{a} = (1/2, \sqrt{3}/2)$, $\sigma = 0$, $h^* = 1/32$, $h = \sqrt{4/3}h^*$, Péclet number $Pe_h \approx 3.60844$, Damköhler number $Da_h = 0$. [Color figure can be viewed in the online issue, which is available at wileyonlinelibrary.com.]

B. Example 2: Boundary and Inner Layers Present

Choose the convection field $\mathbf{a} = (a_1, a_2)^T := (1/2, \sqrt{3}/2)^T$, $f = 0$, $\sigma = 0$, $h^* = 1/32$, and $h = \sqrt{4/3}h^*$. The domain with boundary data indicated is given in Fig. 2. The following Figs. 3 and 4 give the elevation, the contour, and the cut of the finite element solution for $\varepsilon = 10^{-2}$, $\varepsilon = 10^{-6}$, $\sigma = 0$, $h^* = 1/32$. The conclusion is that the proposed method can capture the boundary and inner layers. The captured are wider than the true for the mesh size $h = 1/32$, but, decreasing the mesh size, one can expect that the captured approach the true. The cuts show that the method exhibits high stability.

C. Example 3: Front Problem

In this example, we consider a time-dependent problem containing transport when the time is evolving. This example was considered in Ref. [15]. Let $\Omega = (0, 1) \times (0, 1)$, and $f = 0$, $\varepsilon = 10^{-6}$,

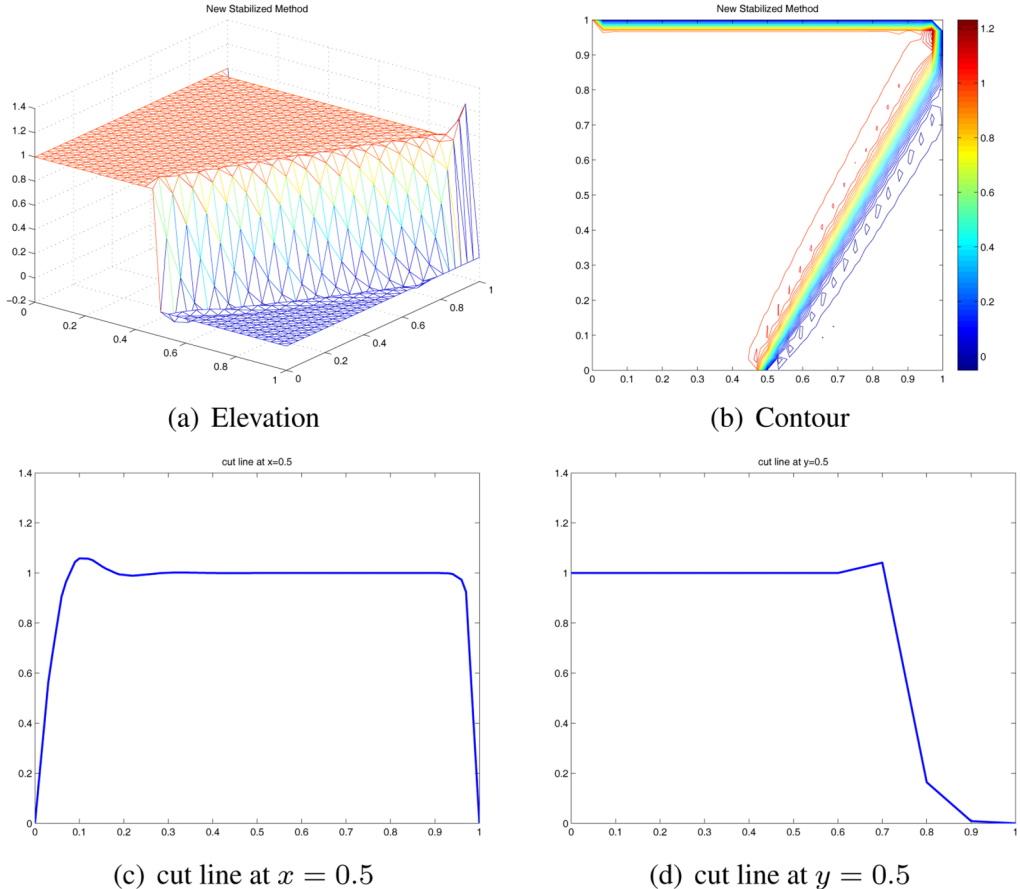


FIG. 4. The elevation, contour, and vertical and horizontal cuts of the finite element solution, with $\varepsilon = 10^{-6}$, $\mathbf{a} = (1/2, \sqrt{3}/2)$, $\sigma = 0$, $h^* = 1/32$, Péclet number $Pe_h \approx 3.60844 \times 10^4$, Damköhler number $Da_h = 0$. [Color figure can be viewed in the online issue, which is available at wileyonlinelibrary.com.]

$\sigma = 0$, and $\mathbf{a} = (\frac{\sqrt{2}}{2}, \frac{\sqrt{2}}{2})^T$. The initial and boundary conditions are described in Fig. 5. For a given $h^* = 1/32$ while $h = \sqrt{2}h^*$, various time steps $\delta t = h^*, h^*/4, h^*/8$, are chosen to produce the stabilized finite element approximations. Since $\sigma h^2 = (\delta t)^{-1}h^2 \gg \varepsilon$, the method is more stable and more accurate, as is shown in the analysis of stability and error estimates. The numerical results at $t = 0.25$ and $t = 1.5$ are, respectively, depicted in Fig. 6. When compared with the results in [15], We can see that the results here are satisfactory.

D. Example 4: Hemker Problem

In this example, we consider the Hemker problem which was considered in Ref. [37]. We use a unstructured mesh which is a nonuniform mesh and make a comparison to SUPG method. From

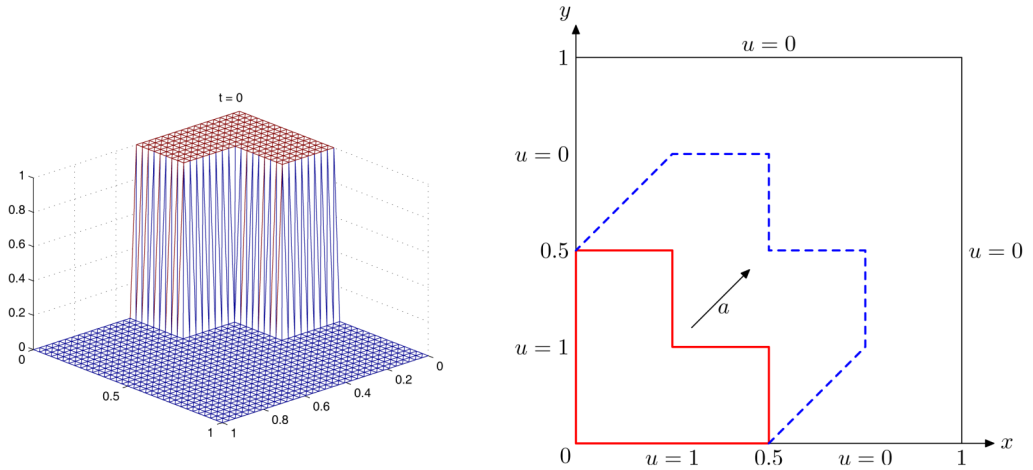


FIG. 5. Initial and boundary conditions of L-shaped front problem. [Color figure can be viewed in the online issue, which is available at wileyonlinelibrary.com.]

the numerical results, we see that the proposed method is suitable for nonuniform meshes and is comparable to SUPG method.

The Hemker problem is given as follows. Let $\Omega = \{[-3, 9] \times [-3, 3]\} / \{(x, y) : x^2 + y^2 < 1\}$, the coefficients are $\mathbf{a} = (1, 0)^T$, $\sigma = 0$, and $f = 0$, and the boundary conditions are given by

$$u(x, y) = \begin{cases} 0, & x = -3, \\ 1, & x^2 + y^2 = 1, \\ \varepsilon \nabla u \cdot \mathbf{n} = 0, & \text{else.} \end{cases}$$

We consider $\varepsilon = 10^{-4}$. We use the *New Stabilized FEM* (6) (P_1 element, #dof=571116) to solve the Hemker problem on a very fine grid. See Fig. 7 for this reference solution with values in the interval $[0, 1]$, from which we can obtain the reference curves for cuts of the solution.

The numerical results are obtained on unstructured meshes of triangular grids, where the level 0 of the unstructured mesh is shown in Fig. 8. Numbers of degrees of freedom for different levels, including Dirichlet nodes, are given in Table VII.

The elevation plots of the New Stabilized FEM solution and the SUPG solution on level 4 are depicted in Fig. 9. We use the cuts of the computed solutions at $x = 4$ and $y = 1$ to study the smearing of the interior layers and the accuracy of the solutions away from the circle, see Fig. 10. To compute of the cut lines at $x = 4$ and $y = 1$, we choose 10001 and 20001 equally distributed points in $y \in [-3, 3]$ and in $x \in [-2, 8]$, respectively. In Fig. 11, the width of the computed interior layers is shown, where only the interior layer at $y = 1$ is plotted, because of symmetry. The width of the interior layer is defined to be the length of the interval $y_{\text{layer,num}} = y_1 - y_0$ in which the solution falls from $u(4, y_0) = 0.9$ to $u(4, y_1) = 0.1$. For the reference solution, $y_{\text{layer,num}}^{\text{ref}} = 0.06$. On Level 3 and Level 4 of the unstructured meshes, we assess the quality of solutions at the layers from the differences to the cut lines at $y = 1$ and $x = 4$, as shown in Figs. 12 and 13, where we compute the differences to reference cut lines in each point and we obtain a vector of errors e . In

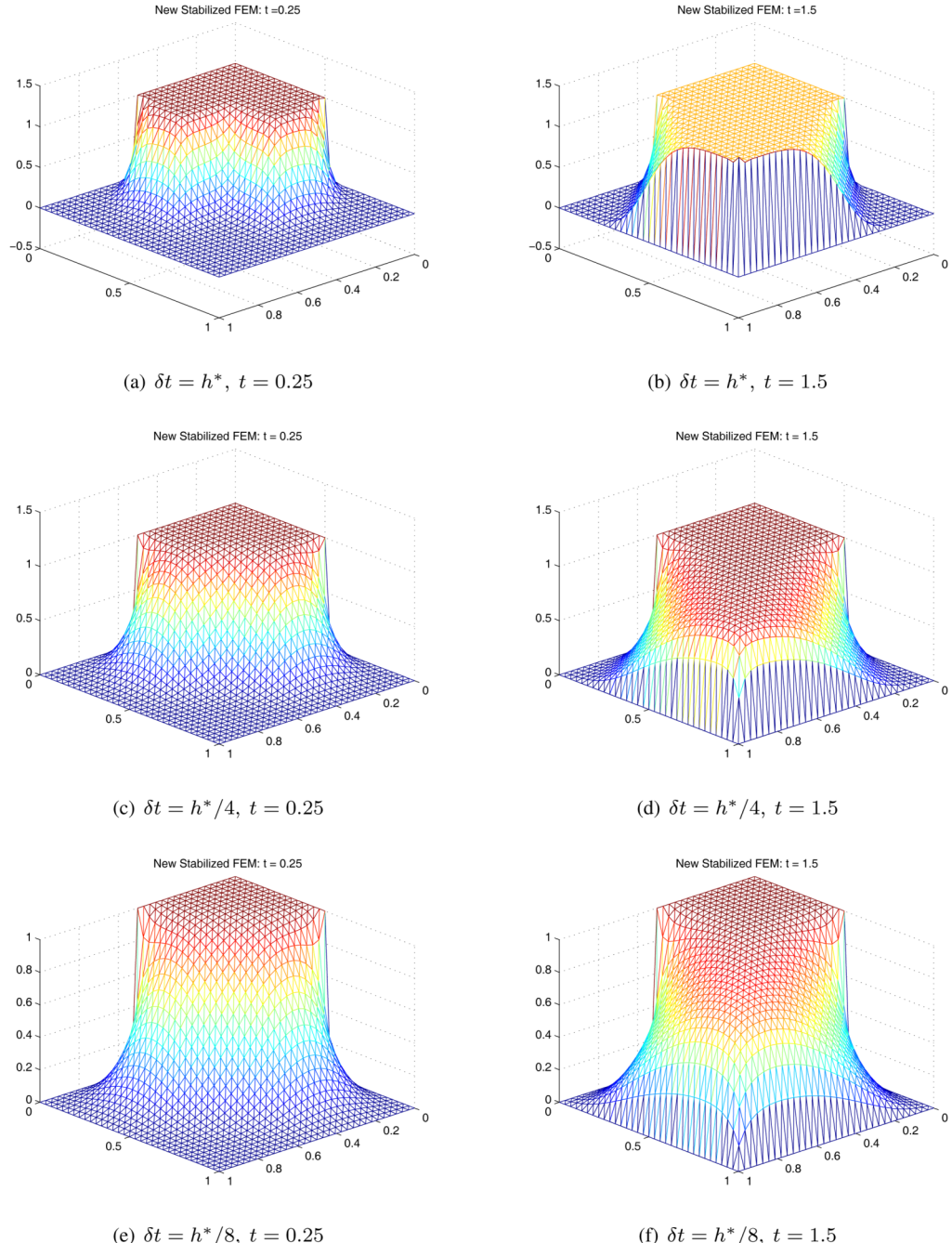


FIG. 6. Elevation plots of the stabilized finite element solutions of L-shaped front problem with $\varepsilon = 10^{-6}$ and $\sigma = 0$ at $t = 0.25$ and $t = 1.5$, using P_1 elements, $h^* = 1/32, h = \sqrt{2}h^*$ and time step $\delta t = h^*$ (top row), $\delta t = h^*/4$ (middle row), $\delta t = h^*/8$ (bottom row). [Color figure can be viewed in the online issue, which is available at wileyonlinelibrary.com.]

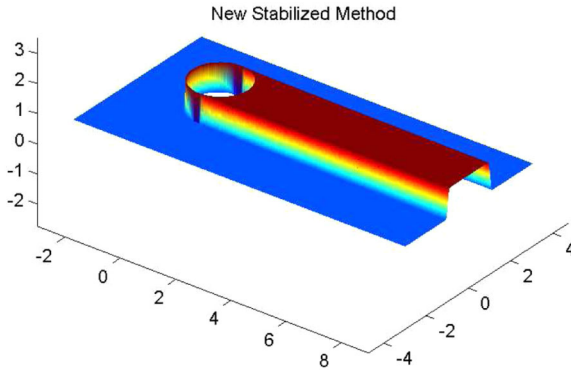


FIG. 7. Solution of the Hemker problem for $\varepsilon = 10^{-4}$. [Color figure can be viewed in the online issue, which is available at wileyonlinelibrary.com.]

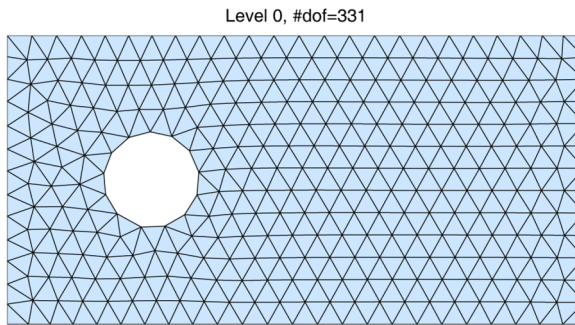


FIG. 8. Hemker problem, unstructured triangular grid(level 0). [Color figure can be viewed in the online issue, which is available at wileyonlinelibrary.com.]

TABLE VII. Hemker problem, numbers of degrees of freedom for different levels.

Level	0	1	2	3	4
#dof	331	1303	5175	20446	81644

both figures, we show the errors in the maximum norm $\|e\|_\infty$ and the averaged Euclidean norm $\|e\|_2 := (n^{-1} \sum_{i=1}^n e_i^2)^{1/2}$.

VII. CONCLUDING REMARKS

In this article, we propose and analyze a new stabilized finite element method for numerically solving the advection-diffusion-reaction equations. The new method augments the standard Galerkin formulation with a new term from the residual of the partial differential equations in the problem. A new stabilization parameter is designed. The new stabilization parameter reasonably incorporates the mesh-dependent Péclet number and the mesh-dependent Damköhler number. These make the

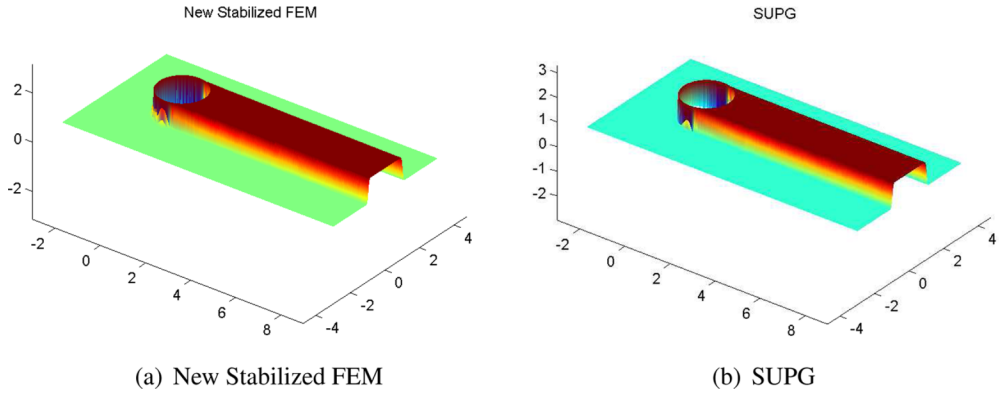


FIG. 9. Hemker problem, the elevation plots of the New Stabilized FEM solution, and the SUPG solution on level 4. [Color figure can be viewed in the online issue, which is available at wileyonlinelibrary.com.]

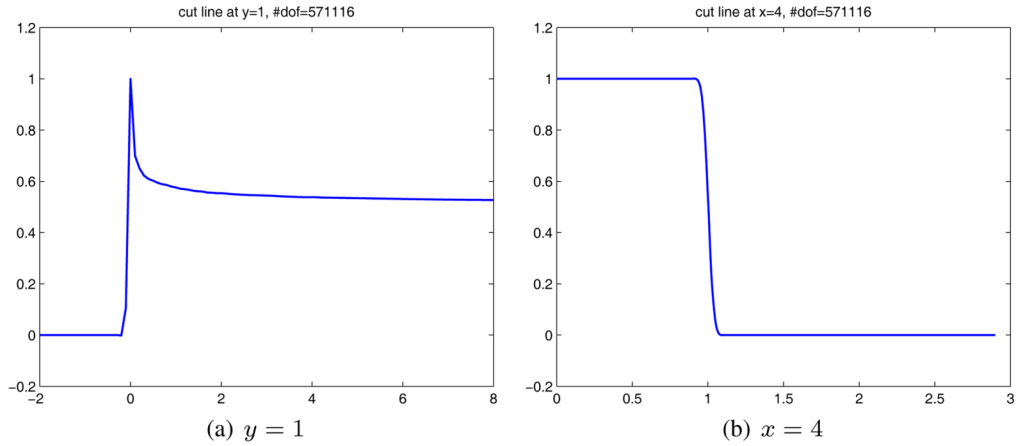


FIG. 10. Hemker problem, cut lines of the reference solution at $y = 1$ and $x = 4$. [Color figure can be viewed in the online issue, which is available at wileyonlinelibrary.com.]

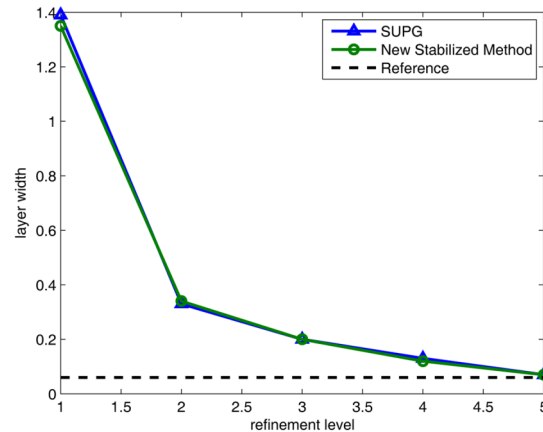


FIG. 11. Hemker problem, layer width at $x = 4$. [Color figure can be viewed in the online issue, which is available at wileyonlinelibrary.com.]

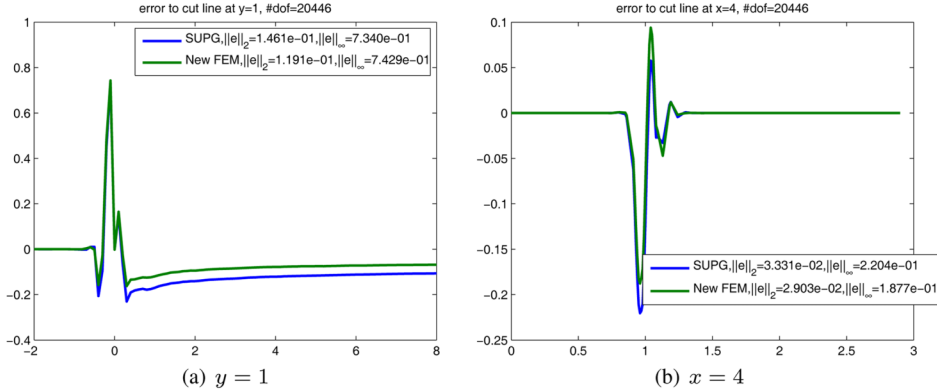


FIG. 12. Hemker problem, errors to reference cut lines at $y=1$ and $x=4$ on Level 3. [Color figure can be viewed in the online issue, which is available at wileyonlinelibrary.com.]

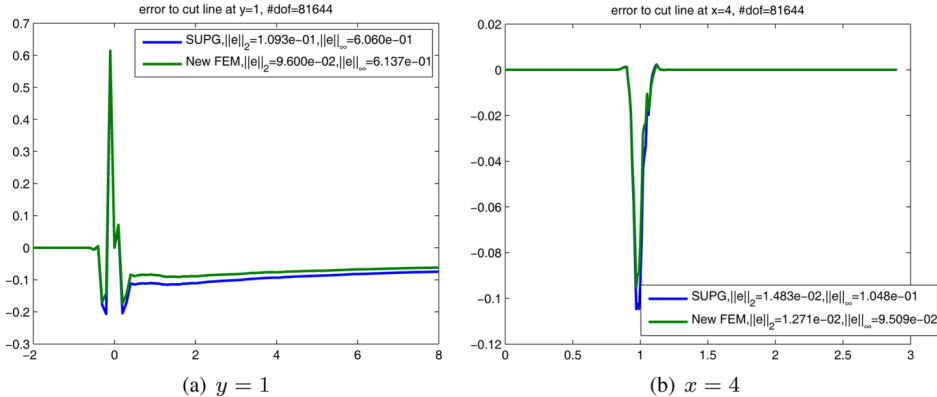


FIG. 13. Hemker problem, errors to reference cut lines at $y=1$ and $x=4$ on Level 4. [Color figure can be viewed in the online issue, which is available at wileyonlinelibrary.com.]

proposed method in this article can well simulate any case of the advection-diffusion-reaction equations. The new method is advantageous over other stabilization methods of the advection-diffusion-reaction equations. This has been justified by theoretical and numerical results. In fact, we have also established the error bounds in H^1 norm and L^2 norm. The dependence on the mesh-dependent Péclet number and the mesh-dependent Damköhler number is explicitly revealed, with respect to ε , σ , $|\alpha|_\infty$ and h , while numerical experiments performed have confirmed the theoretical results and effectiveness of the proposed method.

The authors would like to thank the associate editor and the two anonymous referees for their valuable comments and suggestions which have helped to greatly improve the overall presentation of the paper.

References

1. K. W. Morton, Numerical solution of convection-diffusion problems, Chapman & Hall, London, 1996.
2. H.-G. Roos, M. Stynes, and L. Tobiska, Robust numerical methods for singularly perturbed differential equations, convection-diffusion-reaction and flow problems, Springer-Verlag, Berlin, 2008.

3. M. Stynes, Steady-state convection-diffusion problems, *Acta Numer.*, 14 (2005) 445–508.
4. A. N. Brooks and T. J. R. Hughes, Streamline upwind/Petrov-Galerkin formulations for convective dominated flows with a particular emphasis on the incompressible Navier-Stokes equations, *Comput Methods Appl Mech Eng*, 32 (1982), 199–259.
5. L. P. Franca, S. L. Frey, and T. J. R. Hughes, Stabilized finite element methods: I. Application to the advective-diffusive model, *Comput Methods Appl Mech. Eng* 95 (1992), 253–276.
6. L. P. Franca and S. L. Frey, Stabilized finite element methods: II. the incompressible Navier-Stokes equations, *Comput Methods Appl Mech Eng*, 99 (1992), 209–233.
7. P.-W. Hsieh, and S.-Y. Yang, On efficient least-squares finite element methods for convection-dominated problems, *Comput Methods Appl Mech Eng*, 199 (2009), 183–196.
8. T. J. R. Hughes, Multiscale phenomena: green's functions, the Dirichlet-to-Neumann formulation, sub-grid scale models, bubbles and the origins of stabilized methods, *Comput Methods Appl Mech Eng*, 127 (1995), 387–401.
9. T. J. R. Hughes, L. P. Franca, and G. M. Hulbert, A new finite element formulation for computational fluid dynamics: VIII, the Galerkin/least-squares method for advective-diffusive equations, *Comput Methods Appl Mech Eng*, 73 (1989), 173–189.
10. L. P. Franca,, G. Hauke, and A. Masud, Revisiting stabilized finite element methods for the advective-diffusive equation, *Comput Methods Appl Mech Eng*, 195 (2006), 1560–1572.
11. H. Y. Duan and G. P. Liang, A new stabilized finite element method for solving the Stokes and Navier-Stokes equations. I. The linear case, *J Syst Sci Complex*, 14 (2001), 278–292.
12. H. Y. Duan and G. P. Liang, A new stabilized finite element method for solving the Stokes and Navier-Stokes equations. II. The nonlinear case, *J Syst Sci Complex*, 14 (2001), 399–412.
13. V. John and P. Knobloch, On spurious oscillations at layers diminishing (SOLD) methods for convection-diffusion equations: Part I: A review, *Comput Methods Appl Mech Eng*, 196 (2007), 2197–2215.
14. V. John and P. Knobloch, On spurious oscillations at layers diminishing (SOLD) methods for convection-diffusion equations, Part II: Analysis for P1 and Q1 finite elements, *Comput Methods Appl Mech Eng*, 197 (2008), 1997–2014.
15. M.-C. Hsu, Y. Bazilevs, V. M. Calo, T. E. Tezduyar, and T. J. R. Hughes, Improving stability of stabilized and multiscale formulations in flow simulations at small time steps, *Comput Methods Appl Mech Eng*, 199 (2010), 828–840.
16. V. John and E. Schmeyer, Finite element methods for time-dependent convection-diffusion-reaction equations with small diffusion, *Comput Methods Appl Mech Eng*, 198 (2008), 475–494.
17. L. P. Franca and E. G. Dutra do Carmo, The Galerkin gradient least-squares method, *Comput Methods Appl Mech Eng*, 74 (1989), 41–54.
18. F. Brezzi and A. Russo, Choosing bubbles for advection-diffusion problems, *Math Models Methods Appl Sci*, 4 (1994), 571–587.
19. F. Brezzi, L. P. Franca, and A. Russo, Further considerations on residual-free bubbles for advective-diffusive equations, *Comput Methods Appl Mech Eng*, 166 (1998), 25–33.
20. L. P. Franca, J. V. A. Ramalho, and F. Valentin, Multiscale and residual-free bubble functions for reaction-advection-diffusion problems, *Int J Multiscale Comput Eng*, 3 (2005), 297–312.
21. P.-W. Hsieh and S.-Y. Yang, A novel least-squares finite element method enriched with residual-free bubbles for solving convection-dominated problems, *SIAM J Sci Comput*, 32 (2010), 2047–2073.
22. L. P. Franca and C. Farhat, Bubble functions prompt unusual stabilized finite element methods, *Comput Methods Appl Mech Eng*, 123 (1995), 299–308.
23. H. Y. Duan, A new stabilized finite element method for solving the advection-diffusion equations, *J Comput Math*, 20 (2002), 57–64.

24. H. Y. Duan, P.-W. Hsieh,, R. C. E. Tan,, and S.-Y. Yang, Analysis of a new stabilized finite element method for solving the reaction-advection-diffusion equations with a large reation coefficient, *Comput Methods Appl Mech Eng*, 247–248 (2012), 15–36.
25. G. Hauke, G. Sangalli, and M. H. Doweidar, Combining adjoint stabilized methods for the advection-diffusion-reaction problem, *Math Models Methods Appl Sci*, 17 (2007), 305–326.
26. C. Johnson, Numerical solution of partial differential equations by the finite element method, Cambridge University Press, Cambridge, 1987.
27. I. Harari, Stability of semidiscrete formulations for parabolic problems at small time steps, *Comput Methods Appl Mech Eng*, 193 (2004), 1491–1516.
28. R. A. Adams and J. J. F. Fournier, Sobolev spaces, 2nd Ed., Academic Press, New York, 2003.
29. P. G. Ciarlet, The finite element method for elliptic problems, North-Holland Publishing Company, Amsterdam, 1978.
30. S.C. Brenner and L. R. Scott, The mathematical theory of finite element methods, 3rd Ed., Springer Verlag, New York, 2008.
31. A. Quarteroni and A. Valli, Numerical approximation of partial differential equations, Springer-Verlag, Berlin, 1994.
32. P. Grisvard, Elliptic problems in nonsmooth domains, Pitman Advanced Pub. Program, London, 1985.
33. V. Girault and P.-A. Raviart, Finite element methods for Navier-Stokes equations: theory and algorithms, Springer Verlag, New York, 1986.
34. F. Brezzi, T. J. R. Hughes, D. Marini, A. Russo, and E. Suli, A priori error analysis of a finite element method with residual-free bubbles for advection dominated equations, *SIAM J Numer Anal*, 36(1999), 1933–1948.
35. L. P. Franca and F. Valentin, On an improved unusual stabilized finite element method for the advective-reactive-diffusive equation, *Comput Methods Appl Mech Eng*, 190 (2000), 1785–1800.
36. H. Y. Duan and F. J. Qiu, A new stabilized finite element method for advection-diffusion-reaction equations, Wuhan University, Research Report, 2014.
37. M. Augustin, A. Caiazzo, A. Fiebach, J. Fuhrmann, and V. John, An assessment of discretizations for convection-dominated equations, *Comput Methods Appl Mech Eng*, 200 (2011), 3395–3409.